

2018

Encrusting Sclerobiont Paleoecology and Bioerosion Of Oysters in the Type Campanian (Upper Cretaceous) of Southwestern France

Macy A. Conrad

The College of Wooster, mconrad18@wooster.edu

Follow this and additional works at: <https://openworks.wooster.edu/independentstudy>

 Part of the [Geology Commons](#), and the [Paleontology Commons](#)

Recommended Citation

Conrad, Macy A., "Encrusting Sclerobiont Paleoecology and Bioerosion Of Oysters in the Type Campanian (Upper Cretaceous) of Southwestern France" (2018). *Senior Independent Study Theses*. Paper 8210.

<https://openworks.wooster.edu/independentstudy/8210>

This Senior Independent Study Thesis Exemplar is brought to you by Open Works, a service of The College of Wooster Libraries. It has been accepted for inclusion in Senior Independent Study Theses by an authorized administrator of Open Works. For more information, please contact openworks@wooster.edu.

Encrusting sclerobiont paleoecology and bioerosion of oysters in the Type Campanian (Upper Cretaceous) of southwestern France



by

Macy A. Conrad

Submitted in partial fulfillment of the requirements
of Senior Independent Study
at The College of Wooster

March 2, 2018

Cover Photo:

Photo taken by Dr. Mark A. Wilson, 2017, Aubeterre-sur-Dronne, France.

Abstract

The Campanian Stage of the Upper Cretaceous was established by Henri Coquand in 1857 based on a sequence of richly fossiliferous shallow water carbonates in the Charente and Charente-Maritime departments of southwestern France. One of the most common macrofossils is the gryphaeid oyster *Pycnodonte vesicularis* (Lamarck, 1806), which often forms extensive shell beds. This bivalve lived primarily on soft marly substrates, forming hard substrate islands. They frequently supported sclerobiont communities comprising encrusters (diverse cheilostome and cyclostome bryozoans, foraminiferans, oysters, bivalves, sabellid and serpulid polychaetes, calcareous sponges), borers (the sponge borings *Entobia*, the worm borings *Maeandropolydora* and *Caulostrepsis*, the barnacle borings *Rogerella*, the phoronid borings *Talpina*, the predatory borings *Oichnus*), the ballistic crustacean trace *Belichnus*, and grazers (*Gnathichnus* and *Radulichnus*). Collections of *Pycnodonte vesicularis* from the Late Campanian Biron, Barbezieux and Aubeterre formations (in ascending stratigraphic order) were assembled to study the systematics and paleoecology of the sclerobionts, and describe the bioerosion ichnofauna. These chalky marls record a sequence from deeper to shallower shelf environments. *P. vesicularis* shells from the deeper-water Biron Formation are relatively large and complete, with their encrusting fauna mostly intact and on exterior surfaces, suggesting rapid burial. Shells from the overlying shallower-water and highly bioturbated Barbezieux and Aubeterre formations are typically heavily bioeroded with fragmentary encrusters, pointing to a complex history of colonization on shell exteriors and interiors. The diversity of sclerobionts increases upwards as the depositional environments shallowed, especially for the bryozoans. Part of this diversity

increase may be because of the longer seafloor residence time of the shallower shells, and part may be due to the growing surficial complexity of the bioeroded shell substrates, but most of this diversity increase appears to reflect a rising biological productivity with the shallowing seas. The bioerosion ichnodiversity increases stratigraphically upwards with the shallowing paleoenvironments.

Acknowledgements

This research was made possible by the support of the College of Wooster Geology Department. Special thanks to my advisor, Dr. Mark A. Wilson, for his travel companionship, constructive comments, continued guidance, and passion for bryozoans. Another special thanks to my second advisor, Dr. Meagen Pollock, for helping me with organization, formatting, writing, and time management. I thank Dr. Paul D. Taylor from the Natural History Museum in London for being an excellent guide in France, for sharing his collection of SEM images, and for continuing to be a useful resource throughout the research compilation. Additional thanks to Patricia Taylor for being a wonderful host while collecting specimens in France. Thanks to APEX, Krista Martin, and Patrice Reeder for all of their assistance with the Student Travel Grant that allowed me to present my research at GSA in Seattle, WA.

Table of Contents

Abstract.....	1
Acknowledgements.....	3
Introduction.....	6
Geology of Charente and Charente-Maritime, southwestern France.....	8
The Campanian Stage of southwestern France.....	11
Campanian Stratotype.....	12
Formations and Stratigraphy of the French Campanian	14
The Gimeux Formation.....	16
The Segonzac Formation	17
The Biron Formation.....	17
The Barbezieux Formation.....	18
The Aubeterre Formation.....	18
The Maurens Formation.....	18
Site Locations	20
Caillaud South.....	20
Chemin Aubeterre.....	21
Bonnes.....	22
Plage des Nonnes.....	23
Pointe de Suzac.....	24
Archiac.....	25
<i>Pycnodonte vesicularis</i>	27
Bryozoan Diversity: Order Cyclostomata vs. Order Cheilostomata.....	28
Methods	30
Field Collection.....	30
Lab Work	30
Measures of Diversity.....	32
Results.....	35
Bioerosion of <i>Pycnodonte vesicularis</i>	35
Encrusting Sclerobionts on <i>Pycnodonte vesicularis</i>	39
Encrusting Bryozoans on <i>Pycnodonte vesicularis</i>	42
Discussion.....	45
Encrusting Sclerobiont Paleoecology and Bioerosion.....	45
Encrusting Bryozoan Diversity.....	47

Conclusions.....	49
References Cited.....	50
Appendices.....	53

Introduction

Oyster shells can serve as a surface for sclerobionts, a term used to collectively describe organisms living in or on a hard substrate (Taylor and Wilson, 2002). Bioerosion is the erosion of hard substrates by living organisms, usually in the form of boring, drilling, scraping, or grazing. This bioerosion is represented in the fossil record by various ichnofauna. Encrusting and bioeroding organisms can be beneficial to understanding the paleobiodiversity of past shallow marine communities. Fossil sclerobionts are preserved in situ, which is extremely beneficial in understanding ancient community structures. The gryphaeid oyster *Pycnodonte vesicularis* (Lamarck, 1806) commonly forms extensive shell beds and supports sclerobiont communities. Discovering and interpreting the encrusting sclerobionts and bioerosion on *P. vesicularis* shells from the Campanian (Upper Cretaceous) of France can contribute to the understanding of diversity and paleoecology in shallow marine environments.

Bryozoans are the dominating encrusting sclerobiont on Campanian oysters. Therefore, their diversity as a phylum cannot be overlooked, even at a localized stage level. During the Campanian, the Phylum Bryozoa experienced the beginning of different global diversity trajectories for the orders Cyclostomata and Cheilostomata. While both cyclostome and cheilostome bryozoans diversified in the Late Cretaceous, the cheilostome bryozoans started to dominate around 73 Mya (McKinney and Taylor, 2001). The cyclostomes, which dominated Jurassic and Early Cretaceous assemblages, declined significantly through the Campanian (Lidgard et al., 1993). Concurrently, cheilostome Bryozoa became more prevalent, increasing their mean species diversity, maximum diversity, and variance toward the end of the Cretaceous (Lidgard et al., 1993).

The purpose of this work is to understand the diversity and interactions of encrusters and bioerosion on shells of *P. vesicularis* from the Type Campanian of southwestern France, and to describe the paleoecology of these bryozoan-rich sclerobiont communities and evolutionary turnover from dominating cyclostomes to dominating cheilostomes.

Geology of Charente and Charente-Maritime, southwestern France

The Charente and the Charente-Maritime departments, located in southwestern France, are part of the Nouvelle-Aquitaine administrative region. The departments are situated in the northern part of the Aquitaine Basin, which is a geological province extending along the coast of the Atlantic Ocean (Figure 1). The Aquitaine Basin covers 35,000 square kilometers onshore and is the second largest Mesozoic and Cenozoic sedimentary basin in France (Biteau et al., 2006). The province is characterized by undulating hills across the terrain, except along the western coastal plains, which are relatively flat. The Paris Basin connects in the northeast and the Massif Central is adjacent to the eastern boundary of the Aquitaine Basin. The basin is identified by six main geological provinces, listed from north to south: (1) the Medoc Platform, (2) the Parentis sub-basin, (3) the Landes Saddle, (4) the North Aquitaine Platform, (5) the foreland of the Pyrenees, and (6) the Pyrenean fold-and-thrust belt (Biteau et al., 2006). The Aquitaine Basin is further divided into four sub-basins: the Parentis, the Adour-Arzacq, the Tarbes, and the Comminges (Biteau et al., 2006). The following research presented is concentrated in the Medoc Platform and Parentis sub-basin in the northern region of the Aquitaine Basin.



Figure 1. Highlighted in red is the administrative region of France known as Nouvelle-Aquitaine. This research is focused in the northwestern part of the region (https://en.wikipedia.org/wiki/Nouvelle-Aquitaine#/media/File:Nouvelle-Aquitaine_in_France_2016.svg).

During the Late Paleozoic, the Hercynian orogeny influenced the underlying geology of the Aquitaine Basin as Euramerica and Gondwana collided to form Pangaea. Siliciclastic detrital deposits first appear as alluvial fans develop in the northern Aquitaine Basin during the Lower Triassic (Platel et al., 1999a, 1999b). There were two major transgression and regression cycles divided by a discontinuity during the Late Cretaceous: the first cycle ranging from the Cenomanian – Turonian, and the second ranging from the Coniacian – Maastrichtian (Platel, 1996). After the Coniacian transgression, almost the entire shelf was covered with a chalky to marly facies (Platel, 1996). From the Cenomanian to the Campanian, about 700 meters of chalk was deposited south of the Paris Basin (Chenot et al., 2016). The Late Cretaceous shelf formations range from 300 to 700 meters in total thickness (Platel, 1996). Final regression was

initiated in the Late Campanian after the northern part of the Aquitaine Basin was completely emerged (Platel, 1996).

Today, almost all of the northeastern part of the Aquitaine Basin is covered with forests and low-growing vegetation on poor soil (Platel et al., 1999b). The soil is primarily underlain by sandy-clayey deposits from the Eocene and Oligocene. Valley exposures in the region between Périgueux, Thenon, and Vergt reveal chalky-marly marine deposits from the Late Cretaceous. Only 350 meters of the Cretaceous succession is exposed, while it has an average total thickness of approximately 430 meters (Platel et al., 1999b). The Cretaceous succession consists of chalky-marly carbonates except for the upper formations, which have more calcareous and slightly siliciclastic coastal deposits.

The Campanian Stage of Southwestern France

According to the International Union of Geological Sciences, the Campanian Stage began 83.6 million years ago and ended 72.1 million years ago during the Late Cretaceous (Figure 2). Named after the French commune Champagne, the Campanian was originally defined in 1857 by Henri Coquand, a French geologist and paleontologist. Various authors have revised the French Campanian Stage after Coquand, including Arnaud from 1876-1897, De Grossouvre from 1895-1901, Seronie-Vivien in 1972, and Platel from 1987-1999, all of who contributed research to the current zonation of the stage in France (Figure 3).

System/ Period	Series/ Epoch	Stage/ Age	Age (Ma)
Paleogene	Paleocene	Danian	younger
Cretaceous	Upper/ Late	Maastrichtian	66.0–72.1
		Campanian	72.1–83.6
		Santonian	83.6–86.3
		Coniacian	86.3–89.8
		Turonian	89.8–93.9
		Cenomanian	93.9–100.5
	Lower/ Early	Albian	100.5–~113.0
		Aptian	~113.0–~125.0
		Barremian	~125.0–~129.4
		Hauterivian	~129.4–~132.9
		Valanginian	~132.9–~139.8
		Berriasian	~139.8–~145.0
Jurassic	Upper/ Late	Tithonian	older

Figure 2. A segment of the geologic time scale indicating the Campanian stage (Upper Cretaceous) (Cohen et al., 2013).

This stage is preceded by the Santonian Stage and is followed by the Maastrichtian Stage within the Upper Cretaceous Epoch. Coquand (1857) originally defined the bottom of the Campanian as the unit lying above the Santonian that contains the ammonite *Placenticeras bidorsatum*. The top of the stage ends below the Maastrichtian reef unit containing the *Hippurites radiosus* (Neumann and Odin, 2001).

SANTONIEN	CAMPAN I E N						DORDONIEN	< Champagne charentaise	COQUAND (1856-1860)	
						H G F E D C B	< Aubeterre			
						"Santonien"	CAMPAN I E N	DORDONIEN		
SANTONIEN	CAMPAN I E N					DORDONIEN			ARNAUD (1876-77-87)	
SANTONIEN	CAMPAN I E N					MAESTRICHTIEN			ARNAUD (1897)	
SANTONIEN	CAMPAN I E N inférieur	CAMPAN I E N supérieur				DORDONIEN			DE GROSSOUVRE (1901)	
SANTONIEN	CAMPAN I E N					MAESTRICHTIEN			SERONIE-VIV IEN (1972)	
SANTONIEN	CAMPAN I E N inférieur		CAMPAN I E N supérieur			MAASTRICHTIEN inf.			PLATEL (1987-89)	
		CAMP.1	CAMP.2	CAMP.3	CAMP.4	CAMP.5	Formation de Maurens			
SANTONIEN	CAMPAN I E N inférieur		CAMPAN I E N supérieur				MAASTRICHTIEN inf.			PLATEL 1996
		CAMP.1	CAMP.2	CAMP.3	CAMP.4	CAMP.5	CAMP.6	Tuffeau de Maurens		
SANTONIEN	CAMPAN I E N inférieur		CAMPAN I E N supérieur				MAASTRICHTIEN inf.			PLATEL
Formation de St-Laurent des Combes	Fm de Gimeux	Fm de Segonzac	Formation de Biron	Formation de Barbezieux	Formation d' Aubeterre	Formation de Maurens			Carte Ribérac (1999)	

Figure 3. An evolution of the definition of the French Campanian formations within the Aquitaine Basin (Platel et al., 1999a, Fig. 3).

Campanian Stratotype

The historical stratotype of the Campanian stage, La Grande Champagne, is located in southwest France within the Aubeterre-sur-Dronne commune of the Charente department (Figure 4). The beds originally defined by Coquand (1858) contain macrofossils such as ammonites, brachiopods, echinoids, rudists, asteroids, and belemnites. Ammonites are the best macrofossils to use when comparing geologic sections in other basins to the historical stratotype (Neumann and Odin, 2001). The last occurrence of *Bostrychoceras polyplegum* is associated with younger deposits, while the older beds containing *Nostoceras hyatti* are below the stratotype (Neumann and Odin, 2001). The stratotype also contains many microfossils including benthic foraminifera,

calcareous nannofossils, and dinoflagellate cysts (Coquand, 1858). Ammonites and benthic foraminifera primarily determine the nine different biozones of the French Campanian (Platel et al., 1999a, 1999b).



Figure 4. Modern day map of the Charente-Maritime and Charente departments, highlighting the Campanian stratotype, La Grande Champagne (http://www.routard.com/images_contenu/partir/destination/poitou_charente/carte/poitou_pop.gif, 2017).

Formations and Stratigraphy of the French Campanian

The Campanian Stage of France is characterized by a white to gray chalk, comprised primarily of argillaceous limestone intermixed with varying amounts of flint and glauconite. The clay minerals within the limestone are predominantly from the smectite group, and illite and kaolinite less commonly exist (Platel et al., 1999a). The thickness of these units gradually increases west toward the Atlantic Ocean, ranging from 140 meters thick in the East to 240 meters in the southwest (Platel et al., 1999a).

The Campanian is generally divided based upon micropaleontological data (Andreieff and Marionnaud, 1973; Platel, 1977; Neumann et al., 1983). Nine biozones are classified based upon the association of benthic foraminifera (Neumann et al., 1983). The Lower Campanian consists of biozones CI–CII, the Middle Campanian consists of biozones CIVa, CIVb, and CV, and the Upper Campanian consists of biozones CVI–CVIII (Figure 5) (Vullo, 2005). Other geologists prefer to divide the biozones into the Lower Campanian (biozones CI–CIII) and Upper Campanian (biozones CIVa–CVIII) (Platel et al., 1999a).

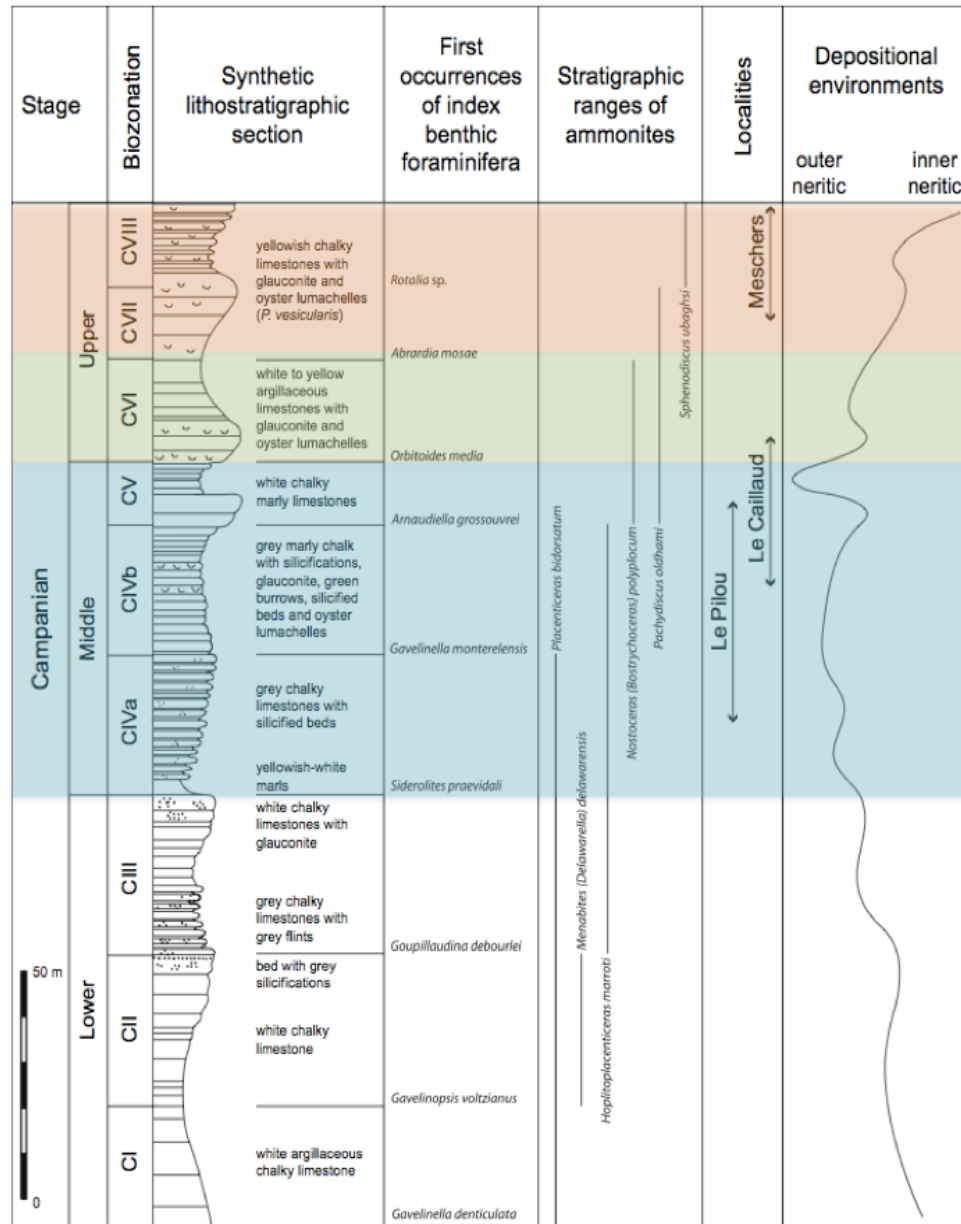


Figure 5. Lower, Middle, and Upper French Campanian biozonation, index fossils, lithology, and transgressions. The formations associated with this research are highlighted: the Biron in blue, the Barbezieux in green, and the Aubeterre in orange (after Vullo, 2005, Fig. 2).

There are six formations within the Campanian Stage of southwest France. In order of oldest to youngest, the formations are: the Gimeux Formation (biozones CI and CII), the Segonzac Formation (biozone CIII), the Biron Formation (biozones CIVa,

CIVb, and CV), the Barbezieux Formation (biozone CVI), the Aubeterre Formation (biozones CVII and CVIII), and the Maurens Formation (biozone CIX) (Figure 6).

C5Ma.	Formation de Maurens (<i>Campanien 6</i>) biozone C IX	Campanien supérieur
C5Au.	Formation d'Aubeterre (<i>Campanien 5</i>) biozones C VII et C VIII	
C5Ba.	Formation de Barbezieux (<i>Campanien 4</i>) biozone C VI	
C5Bi.	Formation de Biron (<i>Campanien 3</i>) biozones C IVa, C IVb, CV	
C5Sg.	Formation de Segonzac (<i>Campanien 2</i>) biozone CIII	Campanien inférieur
C5Gi.	Formation de Gimeux (<i>Campanien 1</i>) biozones C I et C II	

Figure 6. French Campanian formations of the northern Aquitaine Basin (after Platel et al., 1999a, Table 1).

The Gimeux Formation

The Gimeux Formation (Campanian 1) is the lowermost formation overlying the Santonian Stage. Due to the chalky nature, the distinction between the Santonian and Campanian is difficult to determine. However, the Campanian facies are chalkier and is less rich in bryozoans (Platel et al., 1999a). The formation is characterized by a base, middle, and top layer. Generally it transitions from white chalky limestone, to a bed of gray silicification toward the top (Neumann et al., 1983; Neumann and Odin, 2001). The clay content of the base layer is roughly 20% (Platel et al., 1999a). The middle part is comprised of a mixture of wackestone limestone, marly chalk, glauconite, and small,

silicified gray nodules. The top layer has less glauconite and gray silicification, and consists primarily of wackestone limestone.

The Segonzac Formation

The Segonzac Formation (Campanian 2) is a gray chalky limestone with flint intermixed, overlain by white chalky limestone with glauconite (Neumann et al., 1983; Neumann and Odin, 2001). This section alternates between hard and soft limestone. The hard limestone has a clay content of roughly 15% and contains iron sulphide nodules, sometimes staining the clay with rust-colored streaks (Platel et al., 1999a). Both small and large pieces of flint are common throughout the hard facies (Platel et al., 1999a). The soft limestone has a clay content of 20%, with more frequent occurrences of glauconite and less flint (Platel et al., 1999a).

The Biron Formation

The Biron Formation (Campanian 3) is either considered the lone formation of the Middle Campanian or the beginning of the Upper Campanian. Regardless of the distinction and difference in previous literature, the formation begins with a presumed discontinuity (Platel et al., 1999a). This unit is characterized by a yellowish-green mudstone overlain by grey chalky limestone with silicified beds (Neumann et al., 1983; Neumann and Odin, 2001). This transitions into layers of gray marly chalk that includes glauconite, green burrows, silicified beds, and oyster lumachelles (essentially coquina), and has a clay content that exceeds 40% (Neumann et al., 1983; Platel et al., 1999a; Neumann and Odin, 2001). This layer is overlain with more wackestone limestone. The

fauna varies, but bryozoans, sponges, echinoderms, brachiopods, rudist clams, and large benthic foraminifera are common (Platel et al., 1999a). Oysters become particularly abundant in this formation.

The Barbezieux Formation

The base of the Barbezieux Formation (Campanian 4), is similar to the Biron Formation, but only contains 15-20% clay (Platel et al., 1999a). However, the smectites (a group of clay minerals) become scarce as the facies becomes enriched in quartz. Overlying that layer is a gray-white to yellow limestone consisting of clay, glauconite, and oyster lumachelles (Neumann et al., 1983; Neumann and Odin, 2001).

The Aubeterre Formation

The Aubeterre Formation (Campanian 5) is characterized by yellow chalky limestone with glauconite and oyster lumachelles intermixed (Neumann et al., 1983; Neumann and Odin, 2001). This formation corresponds with steep slopes and hillsides where the limestone has been eroded and covered with Paleogene sediments (Platel et al., 1999a). Fine-grained quartz becomes more abundant. At the top of the formation, the limestone is more strongly cemented with a great amount of recrystallization and frequent flint appearances (Platel et al., 1999a). Cephalopods are almost completely absent from this formation (Platel et al., 1999a).

The Maurens Formation

The Maurens Formation (Campanian 6) begins in the Upper Campanian and continues into the Maastrichtian Stage. The last chalk formation is comprised of a couple meters of yellow chalk overlain by white limestone (Platel et al., 1999a). Bryozoans, gastropods, and rudists are common at the end of the Campanian. The appearance of the ammonite *Nostoceras hyatti* marks the beginning of the Maastrichtian and the end of the Campanian Stage.

Site Locations

Caillaud South

Located along the southwest coast of France, Caillaud south (N45° 31.805' W0° 53.629') is an outcrop on the southern side of the commune Talmont-sur-Gironde (Figure 7). The outcrop was situated adjacent to a salt marsh, part of the Gironde Estuary that leads further out to the open Atlantic Ocean (Figure 8). This site was of the Biron Formation, the deepest unit stratigraphically that we collected from. This was the only collection locality within the Biron. Most shell fragments were plucked from the chalky unit, although some specimens had been eroded out of the rock and were found loose along the base of the exposure.

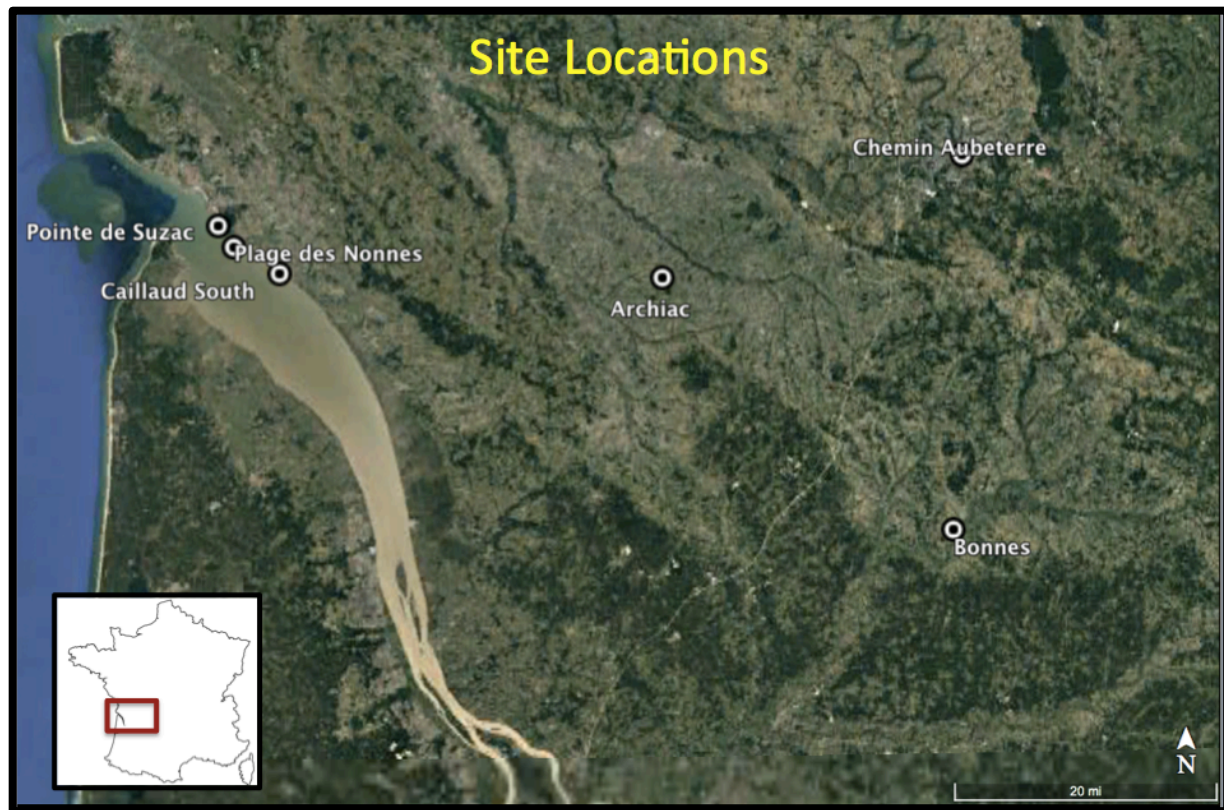


Figure 7. Specimens were collected from 6 different site locations in the Charente and Charente-Maritime departments of southwestern France (Google Earth, Image Landsat/Copernicus).



Figure 8. Dr. Paul Taylor searching for bryozoans within the Biron Formation along the mouth of the Gironde Estuary.

Chemin Aubeterre

Located in the southern part of Aubeterre-sur-Dronne, this site (N45° 16.088' E0° 10.257') was more inland within the Charente department (Figure 7). The outcrop extended up a lane, but was covered in large part by vegetation (Figure 9). Behind the vegetation, there are silicified oyster beds with highly eroded and encrusted shell fragments.



Figure 9. Collecting shells from the Barbezieux Formation at the southern end of Aubeterre-sur-Dronne.

Bonnes

Also situated further inland was an outcrop located just outside the village of Bonnes (N45° 14.735' E0° 08.935') (Figure 7). The outcrop was exposed on both sides of the road, but is becoming increasingly covered with vegetation (Figure 10). Belonging to the Barbezieux Formation, this site was a little more difficult to collect from, but proved to be a significant source of oysters with sclerobiont data.



Figure 10. This oyster-rich road-cutting of the Barbezieux Formation outside Bonnes is quickly becoming overgrown with vegetation.

Plage des Nonnes

The roadcut above Plage des Nonnes (N45° 33.534' W0° 57.895') is another site located along the Atlantic coast (Figure 7). This outcrop of the younger Aubeterre Formation provides a great view of six oyster beds separated by fossiliferous marls (Figure 11). The shells collected here were easily plucked from the outcrop, and some fragments that had been eroded out were collected as well.



Figure 11. The Aubeterre outcrop near the Atlantic coast above Plage des Nonnes shows the extensive and repetitive oyster beds.

Pointe de Suzac

Similar in appearance to Plage des Nonnes, Pointe de Suzac (N45° 34.933' W0° 59.352') is another outcrop along the Atlantic coast (Figure 7). Again of the Aubeterre Formation, this exposure shows the bedding planes of the fossiliferous deposits (Figure 12). Along with oysters, many other fossil fragments were found in the sediments below the oyster beds. The unit contained echinoids, rudists, pectenids, flat bivalves, and was thoroughly bioturbated by *Thalassinoides* shrimp burrows.



Figure 12. Aubeterre oyster beds along the Atlantic coast at Pointe de Suzac.

Archiac

This Aubeterre site was not along the coast, but was situated within the small town of Archiac (N45° 31.413' W0° 17.909') (Figure 7). This outcrop was easily accessible with minimal vegetation cover (Figure 13). Again, prominent oyster beds are exposed and shell fragments can easily be pulled from the marly matrix.



Figure 13. Exposed oyster beds of the Aubeterre Formation in the village of Archiac.

Pycnodonte vesicularis

To research the encrusting sclerobionts and bioerosive activity of the French Campanian, a uniform hard substrate was needed. The gryphaeid oyster *Pycnodonte vesicularis* (Lamarck, 1806) is known for commonly forming extensive shell beds. The calcite shell is well-preserved in the fossil record. *P. vesicularis* is a free-living oyster in soft marine sediments. The life mode of *P. vesicularis* allows sclerobiont colonization equally on both valves pre- and post-mortem.

Almost all of the Campanian oyster shells found were disarticulated, and very few specimens were devoid of bioerosion. Most of the left and right valves showed moderate to heavy bioerosion and sclerobiont encrustation (Figure 14). In addition to bioerosion, the shells were exposed to dissolution and mechanical breaking before burial. The dissolution on some valves is due to the vesicular structure of *P. vesicularis*.



Figure 14. *P. vesicularis*, known for forming extensive shell beds, serves as the hard substrate for encrusting sclerobionts and exhibits bioerosion. This right valve features encrusting bryozoans, and the ichnofossils *Rogerella*, and *Belichnus*.

Bryozoan Diversity: Order Cyclostomata vs. Order Cheilostomata

Prominent encrusters on carbonate shells are bryozoans, marine or freshwater colonial invertebrates. Encrusting colonies are usually composed of runner-like morphologies, or single or multilayered sheets of zooids. Order Cyclostomata is defined by long zooecial chambers and commonly form runner-like, spot-like, or sheet-like colonies (Wyse Jackson, 2010). Order Cheilostomata colonies usually appear in sheets and are composed of box-like zooecia (Wyse Jackson, 2010).

Order Cheilostomata out-diversified Order Cyclostomata for the first time during the Campanian, roughly 73 Mya (Figure 15) (McKinney and Taylor, 2001). While both bryozoan orders diversified in the Late Cretaceous, the cyclostomes began to decline throughout the end of the Cretaceous (Lidgard et al., 1993). Cheilostome bryozoans, however, became more prevalent, increasing their mean species diversity, maximum diversity, and variance toward the end of the Cretaceous (Lidgard et al., 1993). The different diversity trajectories after the Cretaceous extinction could be reflective of differing genera origination rates during the Cenozoic. The cheilostomes diversity is driven more by originations than by extinctions, whereas the history of cyclostomes is driven more by extinctions than by originations (Foote, 2000). The reasoning for the different clade origination rates is largely unknown because the two orders have similar morphologies and thrive in similar ecological conditions. However, cheilostomes have an operculum and are slightly more skeletally complex than cyclostomes (Lidgard et al., 1993). Some cheilostomes have also been known to live in brackish waters and have evolved free-living colonies, both feats that the cyclostomes have not yet developed (McKinney and Taylor, 2001).

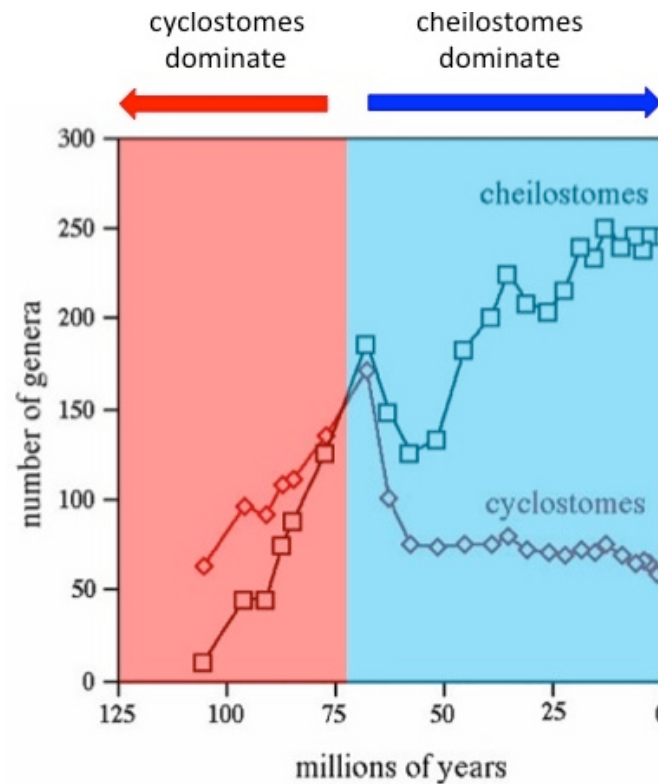


Figure 15. During the Campanian, cheilostomes begin to diversify more than the cyclostomes for the first time and continue to globally dominate as cyclostomes decline throughout the Cenozoic (modified after McKinney and Taylor, 2001).

Pierre A. Gillard (1940) researched the Cretaceous cliffs of the southern coast of the Charente Maritime department, abundant with both cheilostome and cyclostome bryozoans. His research added more species to the list of 60 originally defined specimens at Royan (D'Orbigny, 1852; Canu, 1910; Douvillé, 1910). He also identified a variety of species of cyclostome bryozoans in the compact limestone beds of the Maastrichtian cliffs of the Gironde estuary. His research modified the synonymy of certain species, as well as confirmed the infrequency of some cyclostomes throughout the latter stages of the Cretaceous.

Methods

Field Collection

All 421 shell fragments were collected from the Campanian of southwestern France. There were 6 collection sites located in the Charente and Charente-Maritime departments: 1 site of the Biron Formation, 2 of the Barbezieux, and 3 of the Aubeterre. The sites were chosen based on abundance of samples, collection ease and ability, and prior collection success. At each site, the goal was to collect as many shells as possible with sclerobionts. Therefore, we collected all of the fragments with borings and/or encrusters. Some oyster shells came directly from the marly matrix, while others that had been eroded from the outcrop could be collected from the ground. Almost all bivalve shells of *P. vesicularis* were disarticulated and both right and left valves were collected. From the Biron, 36 shell fragments were collected, 137 were collected from the Barbezieux, and 248 were collected from the Aubeterre.

Once all of the samples made it back to the field station in La Barde, France, each fragment was washed and reexamined for the presence or absence of sclerobionts and/or bioerosion. The samples were carefully packaged according to collection site and formation, and were then sent back to the lab in Wooster, Ohio.

Lab Work

In the Paleontology Lab at the College of Wooster, the specimens were washed again, sorted, and labeled. Every shell fragment was labeled with a code representing the locality it was collected from (Figure 16). Each specimen was given its own tray and a descriptive tag identifying the types of sclerobionts and ichnofossils present. A binocular

Nikon microscope was used to examine each shell at a magnification range of 1.8x to 80x. Each sclerobiont was identified as accurately as possible and sorted into an informal group (bryozoan, bivalve, foraminiferan, polychaete, etc.) or ichnogenus when recognizable.



Figure 16. Campanian oysters labeled with a specific number representing the collection site.

Each specimen was also given a pink tag identifying bryozoans at the genus level (Figure 17). A file of scanning electron microscope (SEM) bryozoan images from Dr. Paul Taylor of the Natural History Museum was very helpful in identifying the encrusting bryozoans. Each bryozoan was identified as accurately as possible, although erosion and lack of SEM examination made some identifications unsure.



Figure 17. Interiors and exteriors of left and right valves of *P. vesicularis* were examined for type and number of sclerobionts and bioerosion. Organized by formation, each box contains a white tag detailing the types of encrusters and ichnofossils on each fragment. The pink tags identify the bryozoans encrusted on the specimen.

Once all of the encrusters and bioerosion had been identified and thoroughly reexamined, the data were collected and input into Microsoft Excel. All sclerobiont tables are available in Appendix B – H.

One specimen from each formation (3 total) was sacrificed in an attempt to attain epoxy casts of microborings. Once the epoxy was fully hardened, the shells were dissolved in dilute hydrochloric acid (10% HCl) for 2 hours. The dilute solution was changed twice. The epoxy casts were cut apart to identify any microborings.

Measures of Diversity

Two measurements of diversity were used to examine the variety of encrusting sclerobionts and bioerosion ichnofauna. The first measure was species richness, which refers to the number of species in a given area or in a given sample (Spellerberg and

Fedor, 2003). Diversity occurs at different scales and levels of taxonomic grouping. In my research, species richness does not refer to the organization of the data at the species level. The bioerosion species richness was calculated at the ichnogenus level. The encrusting sclerobionts were organized into informal groups (such as bryozoans, bivalves, sabellids, sponges, etc.) and then species richness was calculated for each of the informal groups. Species richness for the encrusting bryozoans was calculated at the genus level.

The second measure of diversity used was a measure of species diversity. To account for the total variation of encrusting sclerobionts on the specimens collected, I used Shannon's Index or H (Shannon and Weaver, 1949). Commonly mislabeled as the Shannon-Wiener Index or the Shannon-Weaver Index, H is a measure of information, choice, and uncertainty (Shannon, 1948). The Shannon Index is a widely used index to measure biological diversity (Spellerberg and Fedor, 2003). Additionally, H should be used in situations where rare and abundant species or traits are equally important, where the total variation of the community is desired (Morris et al., 2014).

As a diversity index, the Shannon Index measures how many different individuals are in a community and how evenly the individuals are distributed. The Shannon Index is designed to understand community structure and takes the relative abundances of different species into account. Essentially, H measures how rare and how common species are in a community. The Shannon Index is defined by the following equation:

$$H = - [p_1 \log p_1 + p_2 \log p_2 + \dots + p_n \log p_n]$$

or

(1)

$$H = -\sum p_i \log p_i$$

where

p_n (p_i) represents a set of independent symbols, messages, or organisms. In this research, p_n is the expression of each informal group of encrusting sclerobionts and when defining diversity for the encrusting bryozoans, p_n is the expression of bryozoans at the genus level. The probability of each encruster on the oysters within the given community is expressed as a number less than one. The logarithms of numbers less than one are themselves negative. Therefore, after the sum of the logarithms of the probability of each encruster being present in the community is defined, the sum is multiplied by -1 in order that H be positive (Shannon and Weaver, 1949).

Results

Bioerosion of *Pycnodonte vesicularis*

See Appendix B for the complete bioerosion ichnofauna inventory. There were nine types of bioerosion trace fossils discovered on the Campanian shell fragments (Figure 18). There were five types of borers (Figure 19), two types of predatory traces (Figure 20), and two types of grazing traces (Figure 21). The majority of shell fragments showed at least one type of bioerosion, but several fragments showed multiple types of borings.

There is an increase in ichnofauna diversity from the Biron to Aubeterre Formation (Figure 18). *Entobia* and *Maeandropolydora* borings were present in all formations, and *Gnathichnus* and *Rogerella* were present in the Barbezieux and Aubeterre Formations. *Oichnus*, *Radulichnus*, *Belichnus*, *Caulostrepsis*, and *Talpina* did not appear on the shell fragments until the Aubeterre. The dominant borer was the sponge boring *Entobia*, representing over half of all bioerosion traces.

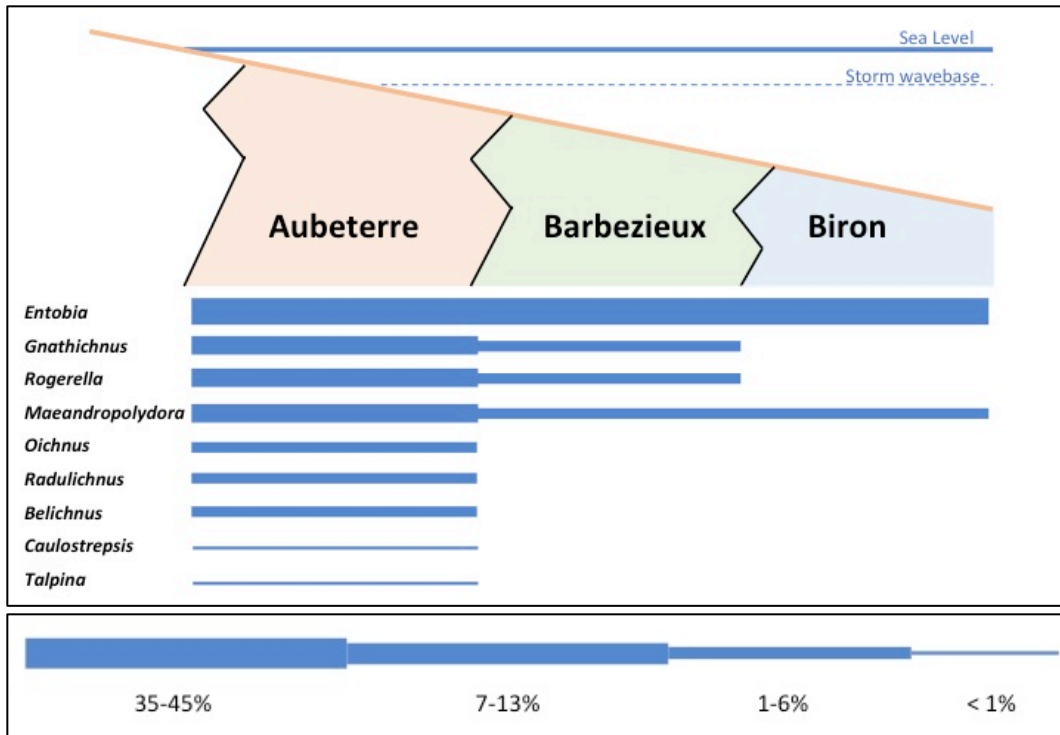


Figure 18. Ichnofauna inventory from 421 Campanian shell fragments of *P. vesicularis*, southwestern France. Each blue bar represents one type of ichnogenus. The thicker the bar, the greater the abundance of that particular trace fossil in each formation. The data organized itself into these four categories. As the environment shallows upwards stratigraphically, the diversity of bioerosion increases.

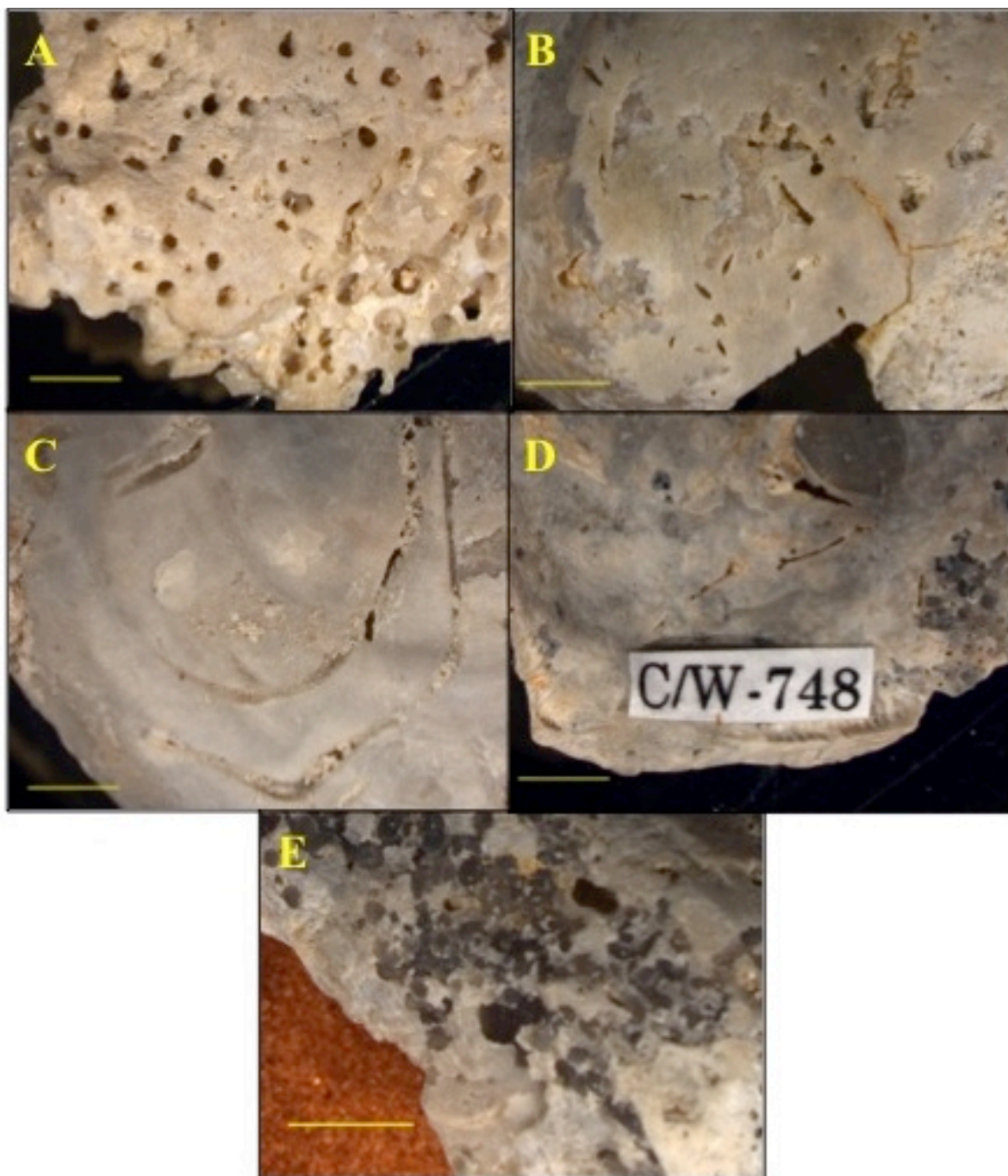


Figure 19. Traces of borers on *P. vesicularis*. **A.** Sponge boring *Entobia*, Plage des Nonnes, Aubeterre Formation. **B.** Barnacle boring *Rogerella*, Plage des Nonnes, Aubeterre Formation. **C.** Polychaete trace *Maeandropolydora*, Pointe de Suzac, Aubeterre Formation. **D.** Phoronid trace *Talpina*, Archiac, Aubeterre Formation. **E.** Worm boring *Caulostrepsis*, Archiac, Aubeterre Formation. Scale bars = 500 μ m.

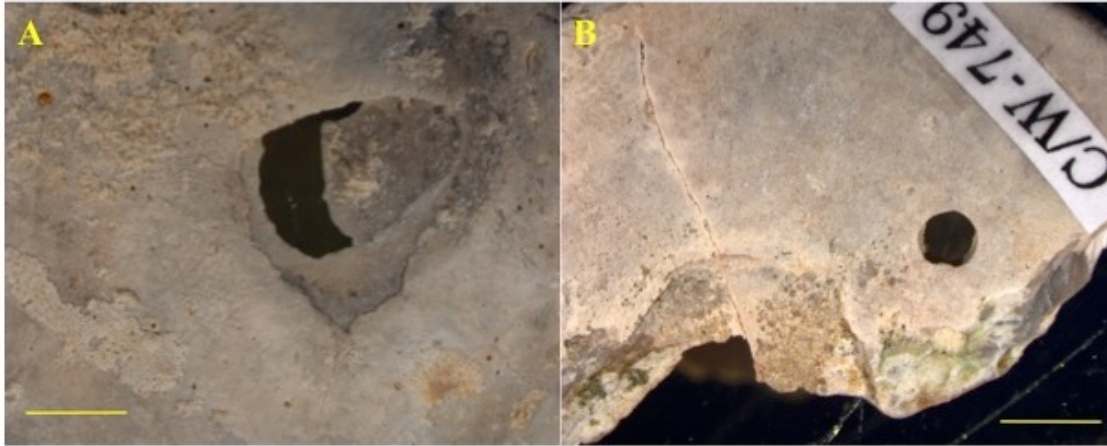


Figure 20. Predatory traces on *P. vesicularis*. **A.** Ballistic crustacean trace *Belichnus*, Archiac, Aubeterre Formation. **B.** Gastropod drill hole *Oichnus*, Pointe de Suzac, Aubeterre Formation. Scale bars = 500 μ m.



Figure 21. Echinoid scraping trace *Gnathichnus*, Archiac, Aubeterre Formation. Scale bar = 500 μ m.

Additionally, the epoxy casts revealed evidence of more borings. The shells did not completely dissolve in the dilute HCl concentration due to high levels of silicification. However, the casts revealed further evidence of sponge borings, and a boring that is only visible inside the valve (Figure 22). Only 3 specimens were dissolved in this process and additional research is needed to interpret the borings occurring within each valve.

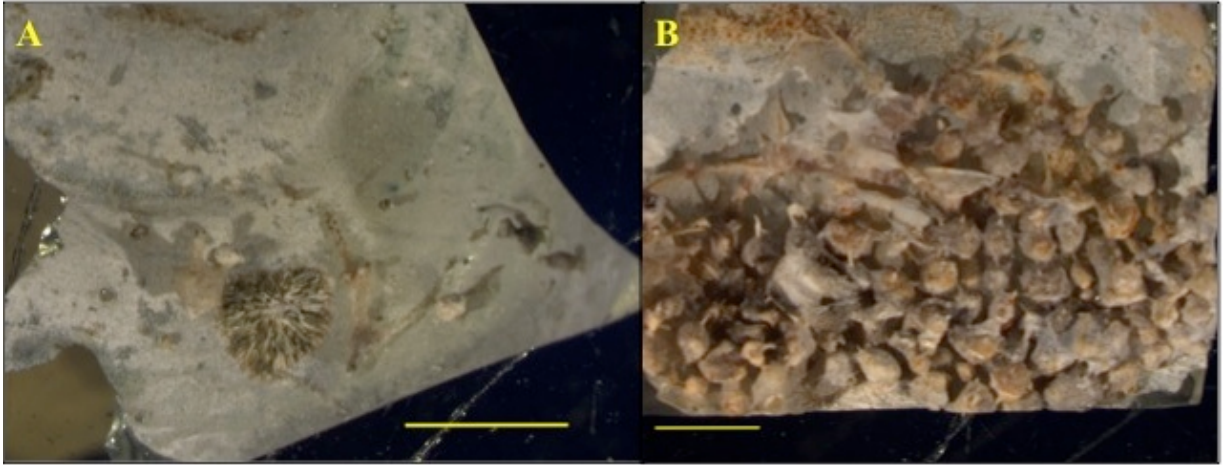


Figure 22. Epoxy casts showing evidence of silicification and the need for further research. **A.** Internal boring not seen on the outside of the shell. **B.** Casts of sponge borings. Scale bars = 500 μm .

Encrusting Sclerobionts on *Pycnodonte vesicularis*

See Appendix C for the complete encrusting sclerobiont inventory. On the 421 shell fragments collected, 7 types of encrusting sclerobionts were found and organized into the following informal groups: bryozoans, bivalves, sabellids, serpulids, foraminifera, sponges, and an unknown encruster (Figures 23 and 24). There is a slight diversity increase in the types of encrusting sclerobionts from the Biron to the Aubeterre (Figure 23). Bryozoans dominated the encrusting assemblages, representing over 60% of all encrusters. Over 85% of all shells in each formation had at least one encrusting bryozoan colony. Fewer had encrusting bivalves, sabellids, foraminiferans, and serpulids. Sponges were only present in the Barbezieux and Aubeterre Formations, while 3 unidentified encrusters were found in the Aubeterre. Although there was an increase in the total types of encrusters, the Shannon Index does not show an increase in total variation going up in the stratigraphic column (Figure 25). Most of the encrusters covered a larger surface area of the shell and were more intact on the Biron oysters, and became more fragmentary on the shells of the Barbezieux and Aubeterre.

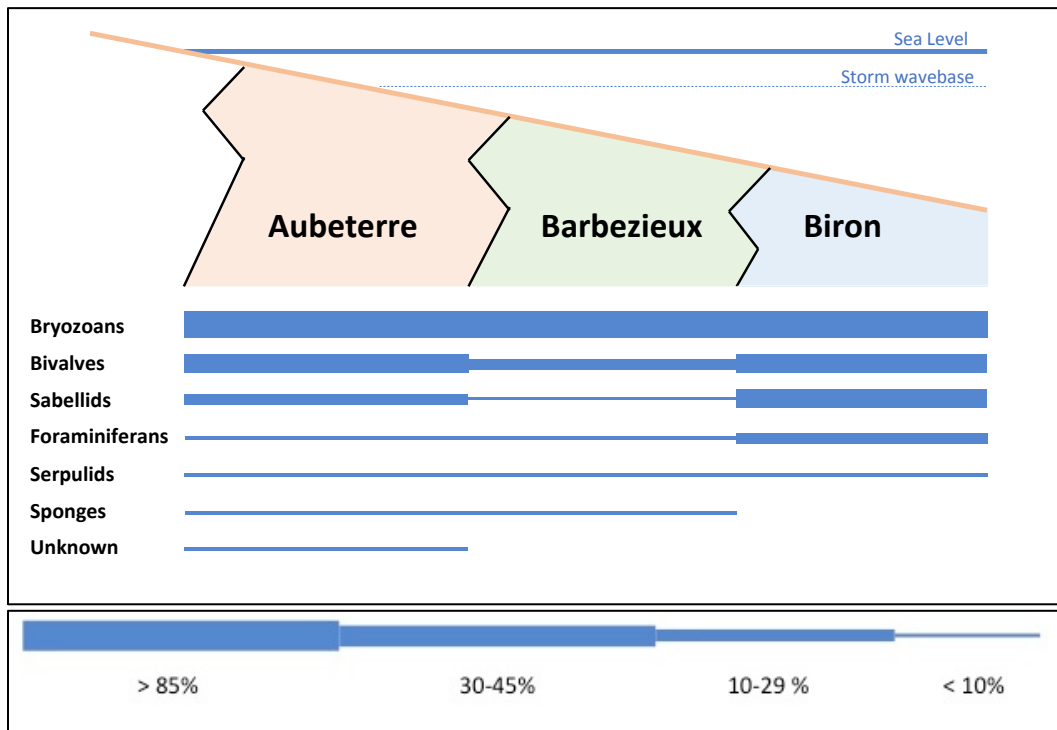


Figure 23. Encrusting sclerobiont data from three Campanian formations of southwestern France. The blue bars represent the percentage of shell fragments collected in each formation with a certain type of encruster. The data organized itself into the four categories with the thicker bars representing a greater proportion of shells encrusted. The diversity of encrusting sclerobionts increases upwards stratigraphically in the Type Campanian. However, the relative abundance of each encruster within each formation does not necessarily increase upwards stratigraphically.

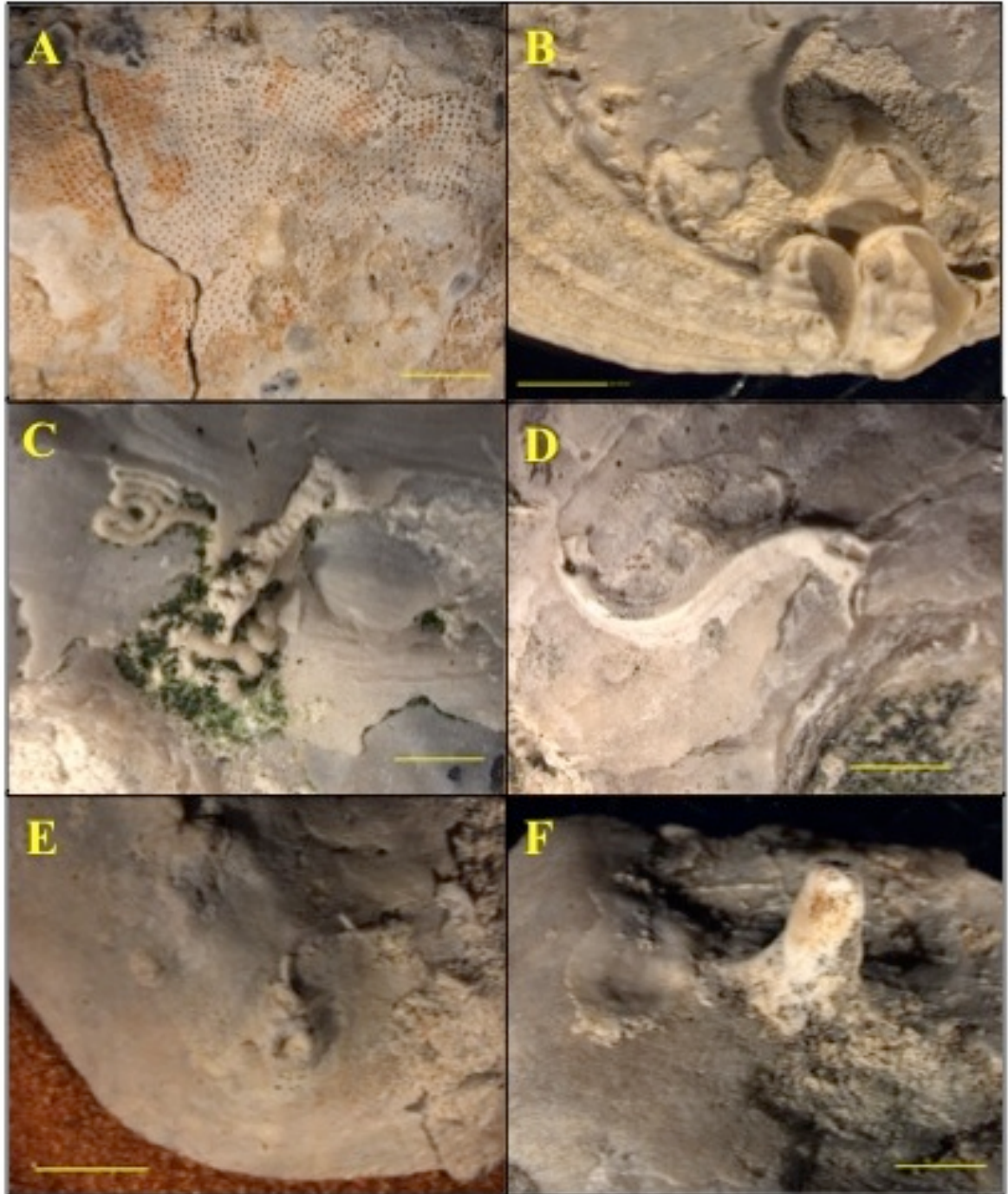


Figure 24. Encrusting sclerobionts on *P. vesicularis* oyster shells. **A.** Bryozoan *Floridina*, Archiac, Aubeterre Formation. **B.** Fixed bivalves, Plage des Nonnes, Aubeterre Formation. **C.** Globular sabellid & encrusting foraminiferans, Caillaud South, Biron Formation. **D.** Polychaete serpulid, Chemin Aubeterre, Barbezieux Formation. **E.** Base of sponge, Pointe de Suzac, Aubeterre. **F.** Unknown encruster, Plage des Nonnes, Aubeterre Formation. Scale bars = 500 µm.

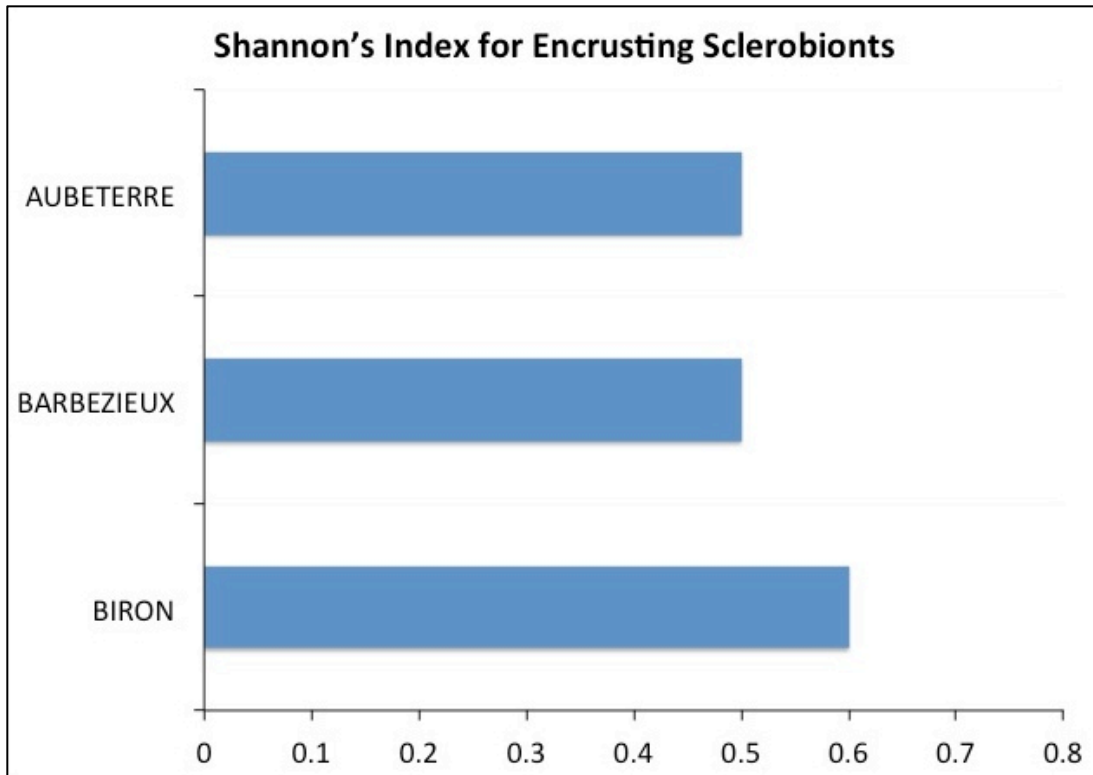


Figure 25. Shannon's Index was calculated for all encrusting sclerobionts on *P. vesicularis* within 3 Campanian formations. The longer the blue bar, the greater the diversity. This measure of diversity alone does not support an increase in diversity in a shallowing upwards sequence.

Encrusting Bryozoans on *Pycnodonte vesicularis*

See Appendices D – H for the complete encrusting bryozoan inventory.

Bryozoans represented over 60% of all encrusting sclerobionts, therefore creating a wealth of data that could be further examined. All encrusting bryozoans were classified at the genus level. From 763 bryozoan colonies, two orders were discovered: Order Cyclostomata and Order Cheilostomata. In ascending stratigraphic order, each formation showed an increase in the total number of individual bryozoan colonies and an increase in the total number of genera (Figure 26). There are more genera of cheilostomes than cyclostomes represented in each formation (Figure 26). The total number of encrusting cheilostome colonies was greater than the number of cyclostome colonies in the Biron

and Aubeterre formations (Figure 27). To accompany the increasing species richness, Shannon's Index shows a slight increase in diversity as the depositional environment shallows (Figure 28). An overwhelming majority of bryozoans (72.7%) were found on the exterior of the valve. Encrustation on the interior of the valve increased from the Biron (9%), to the Barbezieux (12%), and finally to the Aubeterre (39%).

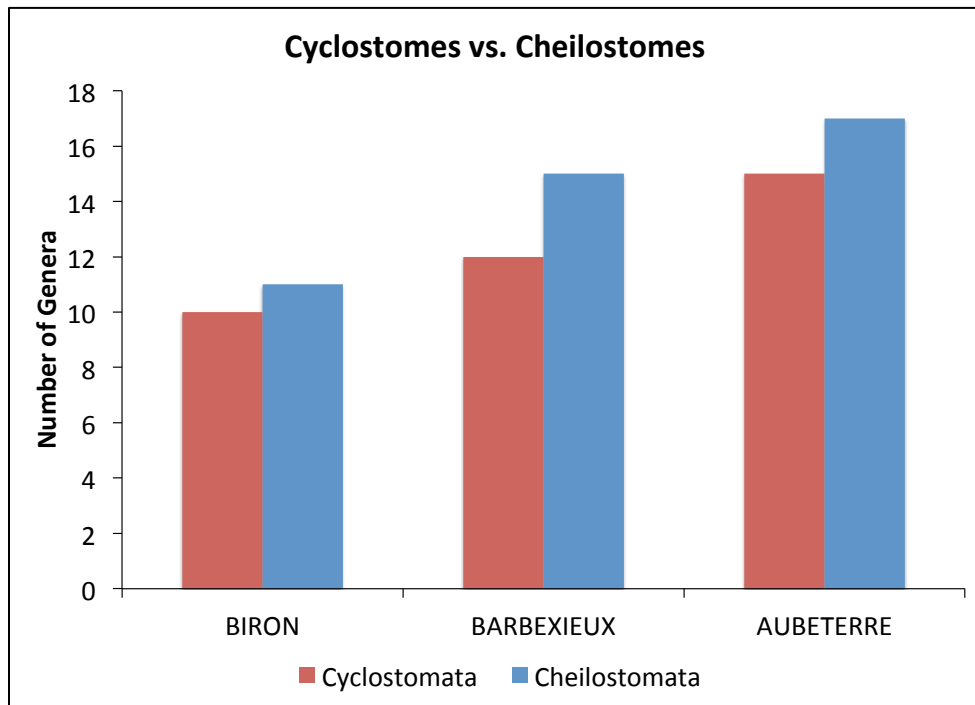


Figure 26. Number of genera of encrusting cyclostome and cheilostome bryozoans on *P. vesicularis* within each studied Campanian formation of southwestern France.

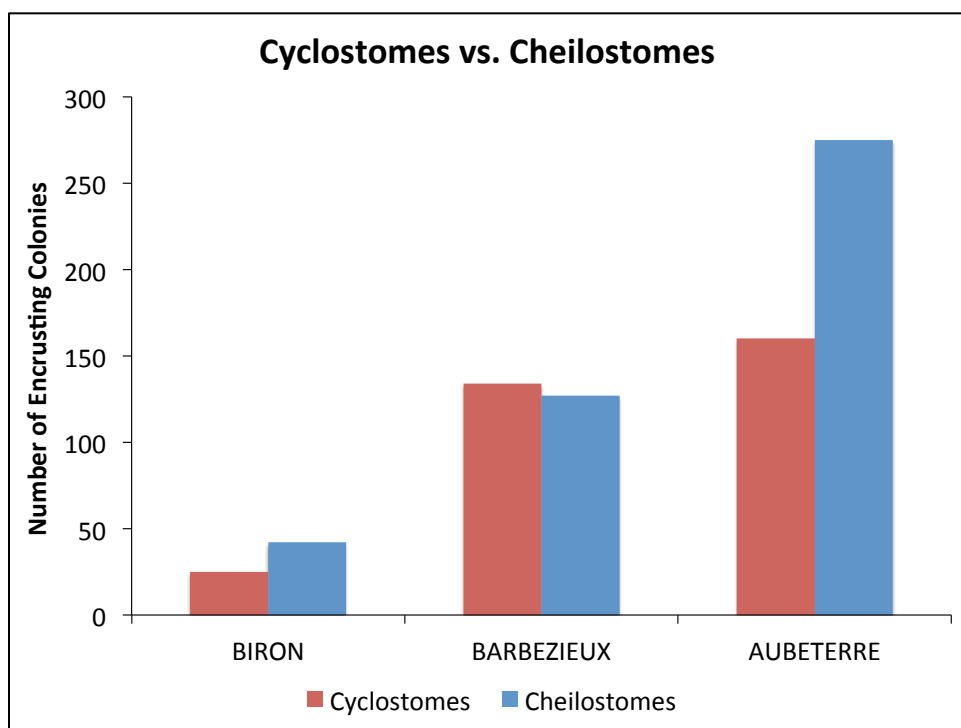


Figure 27. Number of individual encrusting bryozoan colonies on *P. vesicularis* throughout the Campanian formations of southwestern France.

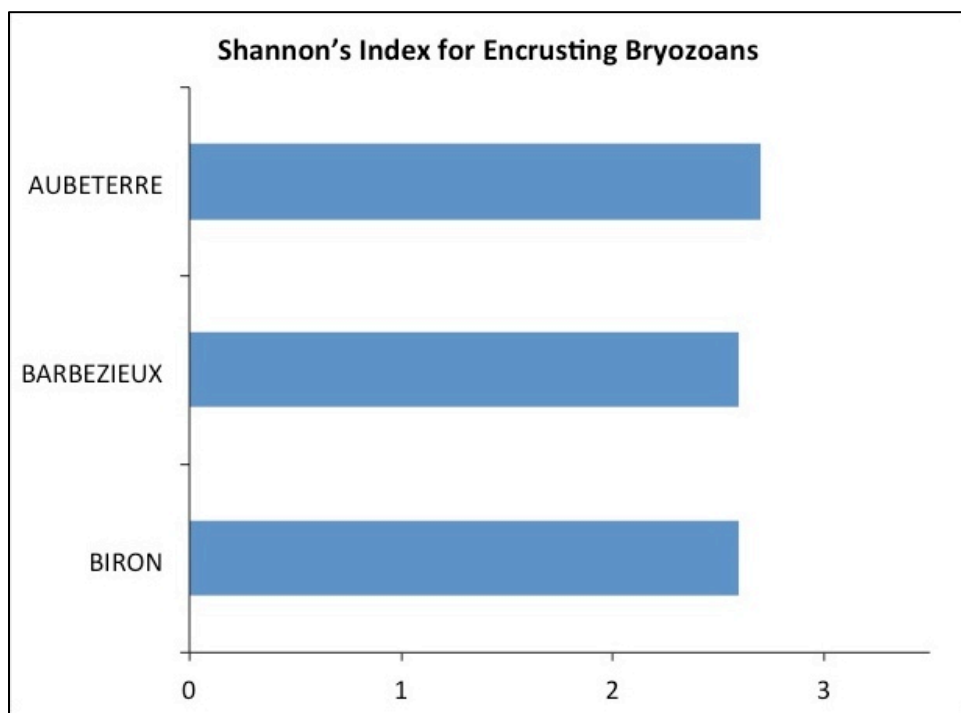


Figure 28. The Shannon Index calculated for the encrusting bryozoans showing a slight increase in total variation in a shallowing upwards stratigraphic sequence. The longer the blue bar, the greater the diversity.

Discussion

Encrusting Sclerobiont Paleoecology and Bioerosion

Ancient communities on hard substrates can be preserved by encrusters that were permanently cemented to the surface, and by borings drilled into the substrate. Benthic marine organisms can attach themselves to organic and inorganic hard substrates in a variety of ways, including organic glue secretions, etching, cementation, secreted holdfasts, and muscular sucker attachment (Bromley and Heinberg, 2006). Additionally, organisms can have different attachment styles (informally named) ranging from permanently affixed, temporarily affixed, periodically mobile, and permanently mobile (Bromley and Heinberg, 2006). Some of these organisms leave trace fossils, while others remain permanently attached. Agostini et al. (2017) suggest that sclerobiont settlement is enhanced by the following factors: higher biofilm bacteria density, surfaces with high ornamentation, shell size, shell texture, heterogeneous internal and external shell surfaces, shallow infaunal or attached epifaunal life modes, and calcitic mineralogy. There are more attachment strategies available for organisms attaching to carbonate substrates than to noncarbonate (Bromley and Heinberg, 2006). Encrustation on the Campanian *P. vesicularis* valves involved temporary attachment through muscular sucker attachment (*Gnathichnus*) and etching (*Entobia*). Permanent attachment was achieved through cementation (sponge spicules) and organic glue secretions from basal membranes (cyclostome and cheilostome bryozoans, foraminiferans, polychaetes, bivalves).

Oyster shells can be bored and encrusted pre- and post-mortem, sometimes revealing the order in which organisms settled on the hard substrate, which describes community dynamics. After death, oyster shells become disarticulated and are

transported to their final place of deposition where the valves can further serve as a hard substrate for sclerobionts and suspension-feeding epibionts. Fossil sclerobionts are preserved in situ, therefore allowing spatial relationships between the substrate and sclerobiont to be retained (Taylor and Wilson, 2003). Any encrustation on the interior of the valves indicates post-mortem encrustation, however it is more difficult to determine if the exterior encrustation was pre- or post-mortem. The ichnofossils *Belichnus* and *Oichnus* were made pre-mortem because they are predatory borings. *P. vesicularis* and boring polychaetes may have a symbiotic relationship, and the *Maeandropolydora* traces may also have been bored pre-mortem. One study showed bioerosive polychaete traces were made parallel to oyster growth lines, indicating they were created during the life of the oyster (Brezina et al., 2014). However, the timing of other borings and encrustation settlements in comparison to the life of the oyster are more difficult to interpret.

Overgrowth interactions can provide insights to the order in which organisms encrusted or bored. Some encrusters had bryozoans growing at the base of attachment, and many bryozoans overgrew existing bryozoan colonies. Therefore, we can conclude that many bryozoans were not the first encrusters on *P. vesicularis* valves. While some bryozoans were bored, many bryozoans and foraminiferans grew in and around existing *Entobia* borings, indicating the demosponge producing the borings was attached to the oyster shell first. This sequence of encrustation has been modeled before on Cretaceous oysters from the Gulf Coast (Bottjer, 1982). Additionally, encrusting foraminifera are known to grow inside pre-existing *Entobia* borings on the interior shell surface (Bromley and Nordmann, 1971).

Similar to other studies of encrustation and bioerosion, the Campanian oysters were encrusted and bored when there was a low sedimentation rate and relatively calm hydrodynamic environment (Bottjer, 1982; Breton et al., 2017). Therefore, encrustation and bioerosion is negatively correlated with high-energy shallow marine environments. However, in order to preserve encrusting organisms attached to a hard substrate directly by cementation, a rapid burial event is necessary (Bromley and Heinberg, 2006). Because the encrusters are so intact in the Biron Formation, a rapid storm event probably buried most of the shell fragments, preserving the sclerobiont settlements. This is supported by the French Campanian stratigraphy showing a regression throughout the Biron, and then an abrupt transgression marking the turnover from Biron to Barbezieux. The preservation of sclerobionts in the other formations is less intact, perhaps indicating a slower burial and longer seafloor residence time. This increased duration of exposure could have led to greater biological activity, which is supported by the increase in abundance and diversity of bioerosion ichnofauna going up in the stratigraphic column from the Biron to the Aubeterre. As the depositional environment shallowed, biological activity was greater and more productive in the shallower marine setting.

Encrusting Bryozoan Diversity

Overgrowth interactions among organisms on marine hard substrates influence community structure and are an expression of competition for space and food. Without overgrowth, it is difficult to interpret the sequence in which the bryozoans encrusted the *P. vesicularis* shell fragments. However, where encrusting sheet-like cheilostomes and runner-like cyclostomes meet, the cyclostomes are consistently overgrown by the

cheilostomes (Lidgard et al., 1993; McKinney, 1993). This overgrowth could be due to the high growth rate of cheilostomes, which could be linked to zooid robustness, as well as cheilostomes generating greater feeding current velocities than cyclostomes (McKinney, 1993). Therefore, cheilostomes both overgrow and deliver nutrient-depleted water to the competing cyclostomes (Lidgard et al., 1993). In this research, there were instances where the cheilostomes grew on top of existing cyclostome runners, and other instances of isolated runners undisturbed by sheet-like colonies. Although it is on a very small scale, these localized overgrowth interactions can support the research suggesting Order Cheilostomata proliferated during the Campanian as Order Cyclostomata declined (Lidgard et al., 1993; McKinney and Taylor, 2001). Additionally, the increase in bryozoan diversity in each formation from shallow to deep supports higher origination rates for cheilostomes than cyclostomes, and supports the hypothesis of a more complex shallow marine community.

Conclusions

The encrusting sclerobionts and bioerosion ichnofauna on Campanian *Pycnodonte vesicularis* oyster shells of the Charente and Charente-Maritime departments of southwestern France add to our understanding of shallow marine community structure. Ichnodiversity and the diversity of sclerobionts increase upwards through the Biron, Barbezieux, and Aubeterre Formations as the depositional environments shallow. Of the encrusters, bryozoans dominated within all fossil assemblages, and this study supports the evolutionary turnover during the Campanian from dominating cyclostomes to dominating cheilostomes. The diversity increase of both encrusting sclerobionts and bioerosion ichnofauna may be due to longer seafloor residence time of the shallower shells and may reflect rising biological activity and productivity with the shallowing paleoenvironments.

Future research is needed to evaluate the sclerobionts at a lower taxonomic ranking. Microboring data should be collected and examined to study the micropaleontology and how it relates to community structure. Additional information is needed on the preferential distribution and spatial abundance of borings and encrusters, and valve maps of the oysters could also prove useful. Data could be divided by site location and compared to formation results to evaluate any trends that occur due to coastal or inland localities. Correlations between particular sclerobionts and ichnofauna should also be studied to better understand the paleobiodiversity of these Campanian formations.

References Cited

- Andreieff, P., and Marionnaud, J.M., 1973, Le Sénonien supérieur des falaises de la Gironde Exemple d'apui de la micropaléontologie à la cartographie géologique: Bulletin du Bureau de Recherches Géologique de France, v. 2, p. 39-44.
- Agostini, V., Ritter, M., Macedo, A., Muxagata, E., and Erthal, F., 2017, What determines sclerobiont colonization on marine mollusk shells?: PLOS ONE, v. 12, doi.org/10.1371/journal.pone.0184745.
- Biteau, J.J., Le Marrec, A., Le Vot, M. and Masset, J.M., 2006, The Aquitaine Basin: Petroleum Geoscience, v. 12, p. 247-273.
- Bottjer, D.J., 1982, Paleoecology of epizoans and borings on some Upper Cretaceous chalk oysters from the Gulf Coast: Lethaia, v. 15, p. 75-84.
- Breton, G., Wisshak, M., Néraudeau, D., and Morel, N., 2017, Parasitic gastropod bioerosion trace fossil on Cenomanian oysters from Le Mans, France and its ichnologic and taphonomic context: Acta Palaeontologica Polonica, v. 62, p. 45–57.
- Bromley, R., and Heinberg, C., 2006, Attachment strategies of organisms on hard substrates: A palaeontological view: Palaeogeography, Palaeoclimatology, Palaeoecology, v. 232, p. 429-453.
- Bromley, R., and Nordmann, E., 1971, Maastrichtian adherent foraminifera encircling clionid pores: Bulletin of the Geological Society of Denmark, v. 20, p. 362-368.
- Brezina, S., Romero, M., Casadio, S., and Bremec, C., 2014, Boring polychaetes associated with *Pycnodonte (Phygraea) vesicularis* (Lamarck) from the Upper Cretaceous of Patagonia. A case of commensalism?: Ameghiniana, v. 51, p. 129-140.
- Canu, F., 1910, Liste des Bryozoaires de la Craie de Royan: Bulletin de la Société Géologique, v. 10, p. 62-65.
- Chenot, E., Pellenard, P., Martinez, M., Deconinck, J., Amiotte-Suchet, P., Thibault, N., Bruneau, L., Cocquerez, T., Laffont, R., Pucéat, E., and Robaszynski, F., 2016, Clay mineralogical and geochemical expressions of the “Late Campanian Event” in the Aquitaine and Paris basins (France): Palaeoenvironmental implications: Palaeogeography, Palaeoclimatology, Palaeoecology, v. 447, p. 42-52.
- Cohen, K., Finney, S., Gibbard, P., and Fan, J., 2013, The ICS International Chronostratigraphic Chart, Episode 36: <http://www.stratigraphy.org/ICSchart/ChronostratChart2016-12.jpg> (accessed March 2017).

- Coquand, H., 1857, Position des *Ostrea columba* et *biauriculata* dans le groupe de la craie inférieure: Bulletin de la Société géologique de France, v. 14, p. 749.
- Coquand, H., 1858, Description physique, géologique, paléontologique et minéralogique du département de la Charente: Besançon, Dodivers, 420 p.
- D'Orbigny, A., 1852, Cours élémentaire de paléontologie et de géologie stratigraphiques: Editions Masson, v. 5, p. 383-848.
- Douvillé, H., 1910, La craie et le Tertiaire des environs de Royan, Bulletin de la Société Géologique de France, v. 4, p. 57.
- Foote, M., 2000, Origination and extinction components of taxonomic diversity: Paleozoic and post-Paleozoic dynamics: Paleobiology, v. 26, p. 578-605.
- Gillard, P., 1940, Sur les Bryozoaires néocrétacés des environs de Royan, pt. 1, Cheilostomata: Société géologique de France, v. 14, p. 14-16.
- Gillard, P., 1940, Sur les Bryozoaires néocrétacés des environs de Royan, pt. 2, Cyclostomata: Société géologique de France, v. 14, p. 59-61.
- Lamarck, J.B., 1806, Mémoire sur les fossiles des environs de Paris: Annales du Muséum d'Histoire naturelle, Paris, v. 8, p. 156-166.
- Lidgard, S., McKinney, F.K., and Taylor, P.D., 1993, Competition, clade replacement, and a history of cyclostome and cheilostome bryozoan diversity: Paleobiology, v. 19, p. 352-371.
- McKinney, F.K., 1993, A faster-paced world?: contrasts in biovolume and life-process rates in cyclostome (Class Stenolaemata) and cheilostome (Class Gymnolaemata) bryozoans: Paleobiology, v. 19, p. 335-351.
- McKinney, F.K., and Taylor, P., 2001, Bryozoan generic extinctions and originations during the last one hundred million years: Palaeontologia Electronica, v. 4, p. 1-26.
- Morris, E., Caruso, T., Buscot, F., Fischer, M., Hancock, C., Maier, T., Meiners, T., Müller, C., Obermaier, E., Prati, D., Socher, S., Sonnemann, I., Wäschke, N., Wubet, T., Wurst, S., and Rillig, M., 2014, Choosing and using diversity indices: insights for ecological applications from the German Biodiversity Exploratories: Ecology and Evolution, v. 4, p. 3514-3524.
- Neumann, M., and Odin, G.S., 2001, Le stratotype historique du Campanien, définition, éléments de corrélation, in Odin, G.S., ed., The Campanian-Maastrichtian Boundary: Elsevier, Amsterdam, p. 677-710.

Neumann, M., Platel, J.-P., Andreiff, P., Bellier, J.-P., Damotte, R., Lambert, B., Masure, E., and Monciardini, C., 1983, Le Campanien stratotypique: étude lithologique et micropaléontologique: *Géologie Méditerranéenne*, v. 10, p. 41-57.

Platel, J.-P., 1977, Le Campanien stratotypique dans le synclinal de Saintes (Charentes): lithostratigraphie, géomorphologie et biozonation: *Bulletin du Bureau de Recherches Géologiques et Minières*, v. 4, p. 261-276.

Platel, J.-P., 1996, Stratigraphie, sédimentologie et évolution géodynamique de la plateforme carbonatée du Crétacé supérieur du nord du bassin d'Aquitaine: *Géologie de la France*, v. 4, p. 33-58.

Platel, J.-P., Célerier, G., Duchadeau-Kervazo, C., Chevillot, C., and Charnet, F., 1999a, Notice explicative, Carte géologie France (1/50 000), feuille Ribérac, Orléans, BRGM, 103 p.

Platel, J.-P., Faugeras, P., Mauroux, B., Spencer, C., Charnet, F., Célerier, G., Harielle, B., and Jacquement, P., 1999b, Notice explicative, Carte géologie France (1/50 000), feuille Thenon, Orléans, BRGM, 128 p.

Shannon, C.E., 1948, A mathematical theory of communication: *The Bell System Technical Journal*, v. 27, p. 379-423.

Shannon, C.E., and Weaver, W., 1949, *The Mathematical Theory of Communication*: Urbana, University of Illinois Press, 125 p.

Spellerberg I.F., and Fedor, P.J., 2003, A tribute to Claude Shannon (1916-2001) and a plea for more rigorous use of species richness, species diversity and the 'Shannon-Wiener' Index: *Global Ecology and Biogeography*, v. 12, p. 177-179.

Taylor, P.D., and Wilson, M.A., 2002, A new terminology for marine organisms inhabiting hard substrates: *Palaaios*, v. 17, p. 522-525.

Taylor, P.D., and Wilson, M.A., 2003, Palaeoecology and evolution of marine hard substrate communities: *Earth-Science Reviews*, v. 62, p. 1-103.

Vullo, R., 2005, Selachians from the type Campanian area (Late Cretaceous), Charentes, western France: *Cretaceous Research*, v. 26, p. 609-632.

Wyse Jackson, P.N., 2010, *Introducing Palaeontology: A Guide to Ancient Life*: Edinburgh, Dunedin Academic Press Ltd, 152 p.

Appendix A – Collection site inventory with College of Wooster locality number and GPS location, color-coded by formation

Location	C/W-###	Unit	Position
Chemin Aubeterre	C/W-745	Barbezieux	N45° 16.088' E0° 10.257'
Caillaud south	C/W-746	Biron	N45° 31.805' W0° 53.629'
Plage des Nonnes	C/W-747	Aubeterre	N45° 33.534' W0° 57.895'
Archiac	C/W-748	Aubeterre	N45° 31.413' W0° 17.909'
Pointe de Suzac	C/W-749	Aubeterre	N45° 34.933' W0° 59.352'
Bonnes	C/W-750	Barbezieux	N45° 14.735' E0° 08.935'

Appendix B – Ichnotaxa inventory with relative abundance (%)

	Aubeterre		Barbezieux		Biron		TOTALS		% of Bioeroded
	# of shells	% of shells	# of shells	% of shells	# of shells	% of shells	# of shells	% of shells	
<i>Entobia</i>	99	40%	48	35%	16	44%	163	38.7%	58.8%
<i>Gnathichnus</i>	31	13%	8	6%			39	9.3%	14%
<i>Rogerella</i>	30	12%	3	2%			33	7.8%	12%
<i>Maeandropolydora</i>	18	7.3%	2	1%	2	6%	22	5.2%	7.9%
<i>Oichnus</i>	8	3%					8	2%	3%
<i>Radulichnus</i>	5	2%					5	1%	2%
<i>Belichnus</i>	4	2%					4	1%	1%
<i>Caulostrepsis</i>	2	0.8%					2	0.5%	0.7%
<i>Talpina</i>	1	0.4%					1	0.2%	0.4%
Total Fragments		248		137		36		421	
Total Bioeroded		198		61		18		277	
% Bioeroded		80%		45%		50%		66%	

Appendix C – Encrusting sclerobiont inventory with relative abundance (%)

	Biron		Barbezieux		Aubeterre		TOTALS		Type of Encruster
	# of shells	% of shells	# of shells	% of shells	# of shells	% of shells	# of shells	% of shells	
Bryozoans	33	92%	131	95.6%	215	86.7%	379	90.0%	60.4%
Bivalves	11	31%	24	18%	111	44.8%	146	34.7%	23.3%
Sabellids	9	30%	11	8.0%	25	10%	45	11%	7.2%
Foraminifera	10	28%	4	3%	18	7.3%	32	7.6%	5.1%
Serpulids	2	6%	5	4%	10	4.0%	17	4.0%	2.7%
Sponges			5	4%	1	0.4%	6	1%	1%
Unknown					3	0.8%	3	0.7%	0.5%
Total Fragments	36		137		248		421		
Total Encrusters	65		180		383		628		

Appendix D – Encrusting bryozoan inventory with relative abundance (%)

	Bron						Barbedieu						Aubetere						Total					
	Internal			External			Internal			External			Internal			External			Internal			External		
	#	% in Fm	#	% in Fm	#	% in Fm	#	% in Fm	#	% in Fm	#	% in Fm	#	% in Fm	#	% in Fm	#	% in Fm	#	% of all	#	% of all	#	% of all
<i>Acrothodes oncostro</i>																								
<i>Actinopora</i>			3	4%	3	4%	3	1%	3	1%	2	0.5%	3	0.7%	5	1%	2	0.3%	3	0.4%	10	1.3%	12	1.6%
<i>Acetmella</i>	1	1%	3	4%	4	6%	17	6.5%	19	7.3%	30	6.9%	46	11%	76	17%	33	4.3%	66	8.7%	99	13%	122	16%
<i>Acanthopora</i>			7	10%	7	10%	2	0.8%	2	0.8%	8	2%	3	0.7%	11	2.5%	10	1.3%	12	1.6%	22	2.9%	22	2.9%
<i>Aplousia</i>			5	7%	5	7%	2	0.8%	4	2%	1	0.2%	1	0.2%	2	0.5%	1	0.1%	8	1%	9	1%	9	1%
<i>Balanastaria</i>													3	0.7%	3	0.7%	3	0.4%	3	0.4%	3	0.4%	3	0.4%
<i>Berenicea</i>			2	3%	2	3%							3	0.7%	3	0.7%	3	0.4%	5	0.7%	5	0.7%	5	0.7%
<i>Bimulticorea variabilis</i>													1	0.2%	1	0.2%	2	0.3%	1	0.1%	1	0.1%	2	0.3%
<i>Bianculligera</i>	1	1	2	3%	3	4%	6	2%	6	2%	3	0.7%	5	1%	8	2%	4	0.5%	13	1.7%	17	2.2%	17	2.2%
<i>Boreasina</i>			1	1%	1	1%							2	0.5%	2	0.5%	2	0.3%	3	0.4%	3	0.4%	3	0.4%
<i>Chirromorph</i>													1	0.2%	1	0.2%	1	0.1%	2	0.3%	2	0.3%	2	0.3%
<i>Diplosolen</i>							1	0.4%	2	0.8%	1	0.2%	1	0.2%	1	0.2%	3	0.7%	1	0.1%	9	1%	10	1.3%
<i>Discospora</i>			4	6%	4	6%	3	1%	3	1%	1	0.2%	2	0.5%	3	0.7%	3	0.7%	1	0.1%	7	0.9%	8	1%
<i>Favospora</i>			5	7%	6	9%	17	6.5%	18	6.9%	11	2.5%	31	7.1%	42	9.7%	13	1.7%	53	7.0%	66	8.7%	66	8.7%
<i>Florida</i>	1	1%	5	7%	6	9%	1	0.4%	1	0.4%	3	0.7%	5	1%	8	2%	4	0.5%	6	0.8%	10	1.3%	10	1.3%
<i>Flustrilora</i>			1	1%	1	1%	1	0.4%	1	0.4%	8	2%	8	2%	16	3.7%	16	2.0%	53	7.0%	69	9.0%	69	9.0%
<i>Idoneus/Pitonea</i>	2	3%	6	9%	8	12%	6	2%	39	15%	45	17%	3	0.7%	5	1%	3	0.4%	3	0.4%	6	0.8%	6	0.8%
<i>Microracella</i>			1	1%	1	1%							17	3.9%	19	4.4%	36	8.3%	19	2.5%	21	2.8%	40	5.2%
<i>Micropora</i>							2	0.8%	2	0.8%	4	2%	1	0.2%	1	0.2%	1	0.1%	3	0.4%	3	0.4%	4	0.5%
<i>Microporid</i>													15	3.5%	18	4.1%	32	7.6%	17	2.2%	31	4.1%	48	6.3%
<i>Nudonysocella</i>			2	3%	2	3%	11	4.2%	13	4.9%	15	3.5%	18	4.1%	32	7.6%	17	2.2%	31	4.1%	48	6.3%	48	6.3%
<i>Oncosacca</i>			2	3%	2	3%	22	8.4%	24	9.2%	16	3.7%	27	6.2%	43	9.9%	18	2.4%	51	6.7%	69	9.0%	69	9.0%
<i>Ophracella</i>			4	6%	4	6%	17	6.5%	19	7.3%	12	2.8%	16	3.7%	28	6.4%	14	1.8%	37	4.9%	51	6.7%	51	6.7%
<i>Ophroporella ramulosa</i>							12	4.6%	12	4.6%			9	2%	9	2%	21	2.8%	21	2.8%	21	2.8%	21	2.8%
<i>Ophiopores neumieri</i>											1	0.2%	1	0.2%	1	0.2%	1	0.1%	3	0.4%	9	1%	12	1.6%
<i>Probesicropora</i>			1	1%	1	1%					3	0.7%	8	2%	11	2.5%	11	1.4%	9	1%	15	2.0%	20	2.6%
<i>Retecora</i>							1	0.4%	1	0.4%	4	0.9%	6	1%	10	2.3%	5	0.7%	1	0.1%	15	2.0%	20	2.6%
<i>Semiliterobrigera</i>			3	4%	3	4%	6	2%	7	3%	3	0.7%	2	0.5%	2	0.5%	2	0.3%	7	0.9%	7	0.9%	8	1%
<i>Scleromicropora</i>			1	1%	1	1%	4	2%	4	2%	2	0.5%	4	1%	6	1%	2	0.3%	6	0.8%	6	0.8%	8	1%
<i>Stomatopora</i>							2	0.8%	2	0.8%	2	0.5%	4	1%	3	0.7%	3	0.4%	2	0.3%	2	0.3%	4	0.5%
<i>Unicore</i>	1	1%	1	1%	2	3%	1	0.4%	5	2%	5	2%	2	0.5%	4	0.9%	3	0.4%	8	1%	11	1.4%	11	1.4%
<i>Unimora</i>							1	0.4%	1	0.4%									1	0.1%	1	0.1%	1	0.1%
<i>Volatopora</i>			1	1%	1	1%	4	2%	25	9.6%	29	11%	20	4.6%	30	6.9%	50	11%	24	3.2%	56	7.3%	80	10%
<i>Wilbertopora</i>			6	9%	6	9%	19	7.3%	25	9.6%	2	0.5%	4	0.9%	6	1%	8	1%	29	3.8%	37	4.9%	37	4.9%
Total encrusting bryozoans	6	9%	61	91%	67	100%	32	12%	229	88%	261	100%	170	39%	265	60.9%	435	100%	208	27.3%	555	72.7%	763	100%

Appendix E – Encrusting bryozoan order inventory (cyclostomes vs. cheilostomes)

	CYCLOSTOMATA			CHEILOSTOMATA			BIRON		BARREUX		AUBERTIERRE	
	Spot	Runner	Sheet	Spot	Runner	Sheet						
<i>Actinopora</i>	X						X	3	X	4	X	5
<i>Berenicea</i>			X				X	2			X	3
<i>Bimulticeps vorabilis</i>			X								X	2
<i>Diplosolen</i>			X						X	1	X	1
<i>Dicrora</i>	X						X	4	X	3	X	3
<i>Fossipora</i>							X		X	5	X	3
<i>Idonaea/Phytonea</i>		X					X	8	X	45	X	16
<i>Microsetella</i>	X						X	1			X	5
<i>Orcosarcia</i>		X					X	2	X	24	X	43
<i>Plethoporella romulosa</i>			X							12	X	9
<i>Protosporopora</i>		X					X	1	X		X	11
<i>Reticularia</i>			X						X		X	
<i>Semiteratubigera</i>			X				X	1	X	4	X	2
<i>Stomatopora</i>	X	X					X		X	1	X	3
<i>Urticora</i>							X	2	X	5	X	4
							X	1	X	29	X	50
<i>Vorticopora</i>		X					X		X	3		
							X	4	X	19	X	76
<i>Acanthodesmia oncostro</i>						X						
<i>Acanthella</i>						X	X					
<i>Acadopora</i>						X		7	X	4	X	11
<i>Acanthopora</i>						X	X		X	2	X	2
<i>Aglaosira</i>						X	X	5	X		X	3
<i>Balanthostoma</i>						X			X	6	X	8
<i>Bivalligera</i>						X	X	1	X	3	X	2
<i>Boreosira</i>						X			X	18	X	42
<i>Cabimorph</i>						X		6	X	1	X	8
<i>Florida</i>						X		1	X		X	36
<i>Fistulifera</i>						X			X	4	X	1
<i>Micropora</i>						X			X	13	X	33
<i>Microporid</i>						X		2	X		X	28
<i>Nudoviridocella</i>						X		4	X	19	X	1
<i>Ovirhynchella</i>						X			X	7	X	10
<i>Rhipidites neuneuri</i>						X		3	X	2	X	6
<i>Sarothecaria simplex</i>						X			X		X	
<i>Sichonicopora</i>						X		6	X		X	
<i>Wittiercopora</i>						X			X	1		
Unknown						X						
Total Bryozoan Genera							21		27		32	
Total Cyclostome Colonies								25		134		160
Total Cheilostome Colonies								42		127		275
Total Colonies in Formation								67		261		435

Appendix F – Encrusting bryozoans of the Biron

BIRON (746)		
Bryozoan	Interior	Exterior
CYCLOSTOMATA		
<i>Actinopora</i>		3
<i>Berenicea</i>		2
<i>Bimulticavea variabilis</i>		
<i>Diplosolen</i>		
<i>Discocavea</i>		4
<i>Favosipora</i>		
<i>Idmonea/Platonea</i>	2	6
<i>Microeciella</i>		1
<i>Oncousoecia</i>		2
<i>Peripora ligeriensis</i>		
<i>Plethoporella ramulosa</i>		
<i>Proboscipora</i>		1
<i>Reptomultelea</i>		
<i>Retecava</i>		
<i>Semilaterotubigera</i>		1
<i>Stomatopora</i>		
<i>Unicavea</i>	1	1
<i>Voigttopora</i>		1
CHEILOSTOMATA		
<i>Acanthodesia ancestra</i>		
<i>Aechmella</i>	1	3
<i>Aeolopora</i>		
<i>Anornithopora</i>		7
<i>Aplousina</i>		5
<i>Balantiostoma</i>		
<i>Batrachopora</i>		
<i>Biaviculigera</i>	1	2
<i>Boreasina</i>		1
<i>Cribrimorph</i>		
<i>Floridina</i>	1	5
<i>Floridinella</i>		
<i>Flustrellaria</i>		1
<i>Membranipora papulata</i>		
<i>Micropora</i>		
<i>Microporid</i>		
<i>Nudonychocella</i>		2
<i>Onychocella</i>		4
<i>Onychocellid</i>		
<i>Pliophloea meunieri</i>		
<i>Porinid base</i>		
<i>Pyriporella</i>		
<i>Semieschara simplex</i>		3
<i>Smittipora</i>		
<i>Stichomicropora</i>		
<i>Wilbertopora</i>		6
OTHER		
Unknown, column thingy		
Unknown, in boring		
Total Encrusting Bryozoa	Interior of valve	Exterior of valve
67	6	61

Appendix G – Encrusting bryozoans of the Barbezieux organized by locality

BARBEZIEUX		
Bryozoan	Interior	Exterior
CYCLOSTOMATA		
<i>Actinopora</i>		
745		3
750		1
<i>Berenicea</i>		
745		
750		
<i>Bimulticavea variabilis</i>		
745		
750		
<i>Diplosolen</i>		
745		
750		1
<i>Discocavea</i>		
745		1
750		2
<i>Favosipora</i>		
745		5
750		
<i>Idmonea/Platonea</i>		
745	6	20
750		19
<i>Microeciella</i>		
745		
750		
<i>Oncousoecia</i>		
745	2	15
750		7
<i>Peripora ligeriensis</i>		
745		
750		
<i>Plethoporella ramulosa</i>		
745		9
750		3
<i>Proboscipora</i>		
745		
750		
<i>Reptomultelea</i>		
745		
750		
<i>Retecava</i>		
745		
750		1
<i>Semilaterotubigera</i>		
745		4
750		
<i>Stomatopora</i>		
745		1
750		

<i>Unicavea</i>		
745		4
750		1
<i>Voigttopora</i>		
745	4	18
750		7
CHEILOSTOMATA		
<i>Acanthodesia ancestra</i>		
745		2
750		1
<i>Aechmella</i>		
745	2	10
750		7
<i>Aeolopora</i>		
745		
750		
<i>Anornithopora</i>		
745	2	1
750		1
<i>Aplousina</i>		
745		1
750		1
<i>Balantiostoma</i>		
745		
750		
<i>Batrachopora</i>		
745		
750		
<i>Biaviculigera</i>		
745		4
750		2
<i>Boreasina</i>		
745		
750		
<i>Cribrimorph</i>		
745	1	1
750		1
<i>Floridina</i>		
745	1	9
750		8
<i>Floridinella</i>		
745		
750		
<i>Flustrellaria</i>		
745	1	
750		
<i>Membranipora papulata</i>		
745		
750		

<i>Micropora</i>		
745	2	2
750		
Microporid		
745		
750		
<i>Nudonychocella</i>		
745	2	7
750		4
<i>Onychocella</i>		
745	2	8
750		9
Onychocellid		
745		
750		
<i>Pliophloea meunieri</i>		
745		
750		
Porinid base		
745		
750		
<i>Pyriporella</i>		
745		
750		
<i>Semieschara simplex</i>		
745	1	4
750		2
<i>Smittipora</i>		
745		
750		
<i>Stichomicropora</i>		
745		2
750		
<i>Wilbertopora</i>		
745	6	13
750		6
OTHER		
<i>Unknown, column thingy</i>		
745		1
750		
<i>Unknown, in boring</i>		
745		
750		
745		
750		
745		
750		
Total Encrusting Bryozoa	Interior of valve	Exterior of valve
261	32	229

Appendix H – Encrusting bryozoans of the Aubeterre organized by locality

AUBETERRE		
Bryozoan	Interior	Exterior
CYCLOSTOMATA		
<i>Actinopora</i>		
747	1	1
748	1	2
749		
<i>Berenicea</i>		
747		1
748		2
749		
<i>Bimulticavea variabilis</i>		
747	1	1
748		
749		
<i>Diplosolen</i>		
747		1
748		
749		
<i>Discocavea</i>		
747		1
748	1	1
749		
<i>Favosipora</i>		
747	1	
748		1
749		1
<i>Idmonea/Platonea</i>		
747	4	3
748	3	4
749	1	1
<i>Microeciella</i>		
747	2	
748	1	2
749		
<i>Oncousoecia</i>		
747	10	9
748	6	17
749		1
<i>Peripora ligeriensis</i>		
747		
748		
749		
<i>Plethoporella ramulosa</i>		
747		4
748		4
749		1
<i>Proboscipora</i>		
747	1	3
748	2	5
749		
<i>Reptomultelea</i>		
747		
748		
749		

<i>Retecava</i>		
747		
748		
749		
<i>Semilaterotubigera</i>		
747		
748		2
749		
<i>Stomatopora</i>		
747	1	
748	1	1
749		
<i>Unicavea</i>		
747	1	1
748		1
749	1	
<i>Voigtopora</i>		
747	9	13
748	10	17
749	1	
CHEILOSTOMATA		
<i>Acanthodesia ancestra</i>		
747		
748		
749		
<i>Aechmella</i>		
747	4	11
748	23	32
749	3	3
<i>Aeolopora</i>		
747		
748		
749		
<i>Anornithopora</i>		
747	1	1
748	7	2
749		
<i>Aplousina</i>		
747	1	1
748		
749		
<i>Balantiostoma</i>		
747		1
748		1
749		1
<i>Batrachopora</i>		
747		
748		
749		

<i>Biaviculigera</i>		
747	2	2
748	1	3
749		
<i>Boreasina</i>		
747		1
748		
749		1
<i>Cribrimorph</i>		
747		
748	1	
749		1
<i>Floridina</i>		
747	2	5
748	9	23
749		3
<i>Floridinella</i>		
747		
748		
749		
<i>Flustrellaria</i>		
747		
748	3	5
749		
<i>Membranipora papulata</i>		
747		
748		
749		
<i>Micropora</i>		
747	5	1
748	12	18
749		
<i>Microporid</i>		
747		
748	1	
749		
<i>Nudonychocella</i>		
747	2	6
748	13	12
749		
<i>Onychocella</i>		
747	5	2
748	7	13
749		1
<i>Onychocellid</i>		
747		
748		
749		
<i>Pliophloea meunieri</i>		
747		
748	1	
749		

Porinid base		
747		
748		
749		
<i>Pyriporella</i>		
747		
748		
749		
<i>Semieschara simplex</i>		
747	1	3
748	1	2
749	2	1
<i>Smittipora</i>		
747		
748		
749		
<i>Stichomicropora</i>		
747	2	2
748		2
749		
<i>Wilbertopora</i>		
747	1	2
748	1	2
749		
OTHER		
<i>Unknown, column thingy</i>		
747		
748		
749		
Unknown, in boring		
747		
748		
749		
747		
748		
749		
747		
748		
749		
Total Encrusting Bryozoa	Interior of valve	Exterior of valve
435	170	265

Appendix I – The Shannon Index (H) for all encrusters

	BIRON	BARBEZIEUX	AUBETERRE
H	0.6	0.5	0.5

Appendix J – The Shannon Index (H) for encrusting bryozoans

	BIRON	BARBEZIEUX	AUBETERRE
H	2.6	2.6	2.7

